# Changes in daily and cumulative volumetric rainfall at various intensity levels due to urban surface expansion over China

*By* DEMING ZHAO[1]*, JINLIN ZHA[1], and JIAN WU[2], [1]*CAS key laboratory of Regional Climate and Environment for Temperate East Asia, Institute of Atmospheric Physics, Chinese Academy of Sciences, Beijing, China;* [2]*Department of Atmospheric Science, Yunnan University, Kunming, China*

## ABSTRACT

Urban surface expansion affects land–atmosphere interactions as well as rainfall. Both the subregional area-averaged daily (DRAIN) and the subregional cumulative volumetric (VRAIN) rainfall amounts are important in this context for hydrological applications and management. Conducted at the city (Beijing, Shanghai, and Guangzhou), city cluster (Beijing–Tianjin–Hebei (BTH), the Yangtze River Delta (YRD), and the Pearl River Delta (PRD)), and national levels in China, numerical experiments were performed in this study using a regional climate model. The analysis revealed that urban-related changes in rainfall variability were more distinct for stronger rainfall among rainfalls of various intensity levels whereas changes in rainfall intensity were more pronounced for weaker rainfall. Furthermore, urban-induced changes in heavy storm rain were more prominent among rainfalls of various intensity levels, for which changes in the variability in DRAIN and VRAIN were more distinct than changes in their intensities, and exhibited marked subregional characteristics. The risk of heavy storm rain increased because of strengthened urban-induced DRAIN and VRAIN variability over Beijing, and urban areas of the YRD and China. However, the risk of heavy storm rain decreased because of decreased DRAIN and VRAIN variability and the reduced intensity of DRAIN over urban areas of Shanghai, nonurban areas of BTH, and nonurban and the entire areas of Guangzhou, the YRD, and the PRD. The urban-induced drying tendency in the lower troposphere and wetting tendency in the low–middle troposphere, and enhanced vertical motions played an important role in determining the changes in DRAIN and VRAIN in case of storm rain and heavy storm rain.

*Keywords: volumetric rainfall amount, daily rainfall amount, urban surface expansion, heavy storm rain, variability*

## 1. Introduction

Anthropogenic factors such as urban surface expansion have been shown to affect the energy and water cycles between the land and atmosphere (IPCC, 2001, 2007, 2013), thereby influencing the climate at the local, regional, and even global scales (Weaver and Avissar, 2001; Inoue and Kimura, 2004; Zhou et al., 2004; Zhao and Wu, 2017), which has attracted increasing interest. Changes in water resources are affected not only by the subregional area-averaged daily rainfall amount (DRAIN) but also the corresponding areas receiving rain and number of rain days, which can be interpreted as the subregional cumulative volumetric rainfall amount (VRAIN). Compared with DRAIN, VRAIN is more important for hydrological and water resource management (McAnelly et al., 1997; Yao and Xu, 2004). Water inflow can be evaluated more concisely based on VRAIN, and is beneficial for forecasting stream flow fluxes, water levels, and flood peaks.

Two strategies have been adopted for evaluating the impact of urban-induced rainfall. The first relies on meteorological station observation data, for which differences between urban and rural areas (Landsberg, 1956, 1970) or within and upwind and downwind of a city (Changnon, et al. 1981, 1991; Diem, 2008; Keuser, 2014) were considered attributable to urbanisation. However, many stations regarded as 'rural' have been affected to some degree by the rapid urbanisation occurring in China

*Corresponding author. e-mail: zhaodm@tea.ac.cn

**1**

over the past 30 years, which makes the 'real' rural stations difficult to determine. In addition, the inhomogeneous meteorological data due to site relocations and instrumentation changes also exerts a considerable influence on the observed values (Yan et al., 2010). The size of wetting correction comprises up to 40% due to the gauge change (Groisman et al., 1975). Furthermore, the evaluated urban-induced changes in rainfall may be overestimated or underestimated owing to the large spatial heterogeneity of rainfall and the discontinuous spatial distribution of meteorological observation stations. The second strategy relies on satellite-based rainfall data such as those from the Tropical Rainfall Measuring Mission (TRMM, Shepherd et al., 2002). Doppler radar data (Mote et al., 2007) and nighttime light data have also been adopted in urban-induced rainfall studies to more accurately detect urban and rural surfaces (Ma and Zhang, 2015).

Zhang et al. (2014) showed the influence of urban surface expansion on the spatial variability of rainfall using data from meteorological stations, weather radars, and the TRMM. However, because of the large spatial heterogeneity of rainfall, using data only from discrete meteorological stations can introduce errors in DRAIN, mean rain areas, and number of rain days, and consequently in VRAIN, with respect to the continuous rainfall data in both the spatial and the temporal dimensions. This is especially pertinent to studies on how urban surface expansion influences rainfall. The urban-induced rainfall may thus be overestimated or underestimated, particularly for periods prior to the widespread use of automated stations. Meanwhile, the relatively recent introduction of satellite-based rainfall data, which can be traced back to only 1997, limits studies over longer periods (Shepherd et al., 2002). Nested dynamical downscaling approaches can provide fine values of the rainfall amount (Gao et al., 2006) reflecting urban land-use changes at both the city and national levels, as well as continuous values in both the spatial and temporal dimensions (Lin et al., 2008), which could help to compute and compare DRAIN and VRAIN values.

In some previous studies, the amount of rainfall was reported to increase over and downwind of cities (Burian and Shepherd, 2005; Baik et al., 2007), whereas no urban-induced rainfall was detected over large cities in Turkey (Tayanc et al., 1997). Therefore, there exist contradictory findings and considerable uncertainty regarding urban-induced rainfall, necessitating further analysis of data measured using gauge stations and satellite-derived or radar-retrieved data in addition to fine-resolution dynamical approaches.

Numerous previous studies have focused on urban-induced rainfall, but the majority of analyses and numerical experiments were performed for single cities or city clusters (Jiang and Tang, 2011; Niyogi et al., 2011; Zhong et al., 2017). With the economic development during the past several decades, China has experienced rapid urbanisation. Marked urban surface expansion has been detected in China, especially over East China. The climate over East Asia (including East China) features a typical monsoon characteristic, namely the East Asian Monsoon (EAM) (Fu, 1997). The impacts of urban surface expansion are concentrated not only in a single city or city cluster, but also are evident throughout the EAM region (Chen et al., 2016; Ma et al., 2016; Zhao and Wu, 2018). Furthermore, studies on urban-induced changes have been conducted in terms of the total rainfall as well as its levels of intensity (Kishtawal et al., 2010; Niyogi et al., 2017), but the results have been obtained mostly based on observation data from inhomogeneous meteorological stations, from which the mean rain areas are challenging to accurately identify. In this article, urban-induced changes in VRAIN and DRAIN for various intensity levels of rainfall are examined using modelling-based continuous values in both the spatial and the temporal dimensions.

In the present study, the nested fifth-generation Penn State/NCAR Mesoscale Model version 3.7 (MM5V3.7) (Grell et al., 1994) was adopted to perform numerical experiments on urban-induced changes in rainfall at various intensity levels at different spatial scales. The default fixed-in-time urban data in the model were replaced by satellite-derived data, with which urban distributions and expansions can be reproduced more accurately (He et al., 2013; Jia et al., 2014; Hu et al., 2015).

## 2. Experimental design and data

The numerical experiments used here were similar to those used by Zhao and Wu (2017; Supplemental Online Material: material and methods). The coarse mesh covered East Asia at a 30-km resolution. The first nested domain covered east China at a 10-km resolution, and the second nested domain covered the three city clusters [Beijing–Tianjin–Hebei (BTH), the Yangtze River Delta (YRD), and the Pearl River Delta (PRD)] at a 3.3-km resolution. The model domain and distributions of the terrain with nested domains (the BTH, YRD, and PRD), and the three cities (Beijing, Shanghai, Guangzhou) are shown in Fig. S1 (see Supplemental Online Material: materials and methods). The land-use data displaying urban surface expansion in China for the years 1980 (U80) and 2010 (U10), and shown in Fig. S2 (see Supplemental Online Material), were employed in the study. Two experiments were performed based on similar model parameters with the exception of the urban distribution, within which U80 and U10 were used separately.
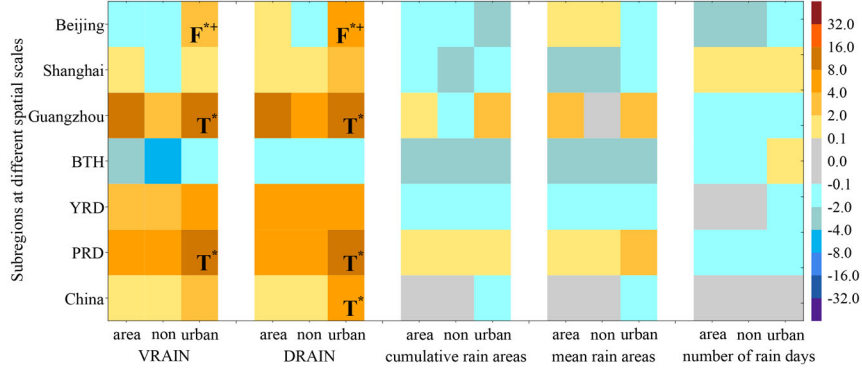
*Fig. 1.* The urban-induced relative changes in total rainfall at different scales. Changes in VRAIN, DRAIN, cumulative rain areas, mean rain areas, and numbers of rain days for total rainfall due to urban surface expansion over nonurban areas (non), urban areas, and subregions as a whole between U80 and U10 (color bar indicates changes. *Indicates passing 95% confidence level significance $F$ tests ($^F*$) or $t$ tests ($^T*$), and $^{F*+}$ and $^{F*-}$ denote enhanced and weakened variability respectively, units: %). Subregions showing significant changes in the variability (intensity) only are marked using $^F*$ ($^T*$), and subregions expressing significant changes in both variability and intensity are marked using $^F*$ and $^T*$.

The definition of urban-induced changes (contribution) to VRAIN was similar to that in a previous study on urban-induced changes in surface air temperature:

$$\text{Contribution} = (R_{U10} - R_{U80})/R_{U10} \times 100\%$$

where $R_{U80}$ and $R_{U10}$ are the values of VRAIN under U80 and U10, respectively. The contributions to DRAIN, cumulative rain areas, mean rain areas, and number of rain days from urban surface expansion are defined similarly, where

$$\text{Cumulative rain areas} = \text{mean rain areas} \times \text{number of rain days.}$$

According to the criteria of the China Meteorological Administration (CMA), DRAIN values can be categorised as five intensity levels based on their intensity: light (0.1–9.9 mm day$^{-1}$), moderate (10–24.9 mm day$^{-1}$), heavy (25–49.9 mm day$^{-1}$), storm (50–99.9 mm day$^{-1}$), and heavy storm ($\geq$100 mm day$^{-1}$).

To explore urban-induced changes in total rainfall and rainfall of various intensity levels, relative changes in the values of VRAIN and DRAIN over different subregions, including nonurban areas and urban areas (areas classified as urban surface in U80 or U10) at different spatial scales were analysed. Significance tests ($F$ tests and $t$ tests) were then conducted to detect the significance of the urban-induced changes in VRAIN and DRAIN. The $F$ tests expressing the significance of changes in the variability are performed based on the variance ratio of the simulated values between U80 and U10, which is similar to that adopted by Hayashi ([1982]). The $t$ tests evaluating the significance of changes in the intensity are conducted using the ratio of mean difference to standard deviation between U80 and U10, which is similar to that applied by Chervin and Schneider ([1976]). Here, '*' indicates

higher than a 95% confidence level on $F$ tests ($^F*$) or $t$ tests ($^T*$), denoting significant changes in the variability and intensity of rainfall, respectively, and $^{F*+}$ and $^{F*-}$ indicate enhanced and weakened variability, respectively. Subregions showing significant changes in the variability (intensity) only are marked using $^F*$ ($^T*$) only, and subregions expressing significant changes in both the variability and the intensity are marked using $^F*$ and $^T*$.

## 3. Results

### 3.1. Urban-induced changes in total rainfall

The urban-induced relative changes in total rainfall (Fig. 1) show that the DRAIN and VRAIN variability strengthened over the urban areas of Beijing, whereas their intensities increased over urban areas of Guangzhou and the PRD. Overall, only the DRAIN intensity increased over the entirety of China. Both the strengthened DRAIN and the expanded cumulative rain areas contributed to the enhanced VRAIN over the urban areas of Guangzhou and the PRD. The mean rain areas expanded but the numbers of rain days decreased, demonstrating that the contributions to the increased cumulative rain areas from the mean rain areas were larger than those from the decreased numbers of rain days. However, the strengthened DRAIN and the decreased cumulative rain areas contributed to the strengthened VRAIN over the urban areas of Beijing and China as a whole, showing that the contributions to the VRAIN from the enhanced DRAIN were larger than those from the decreased cumulative rain areas. Both the mean rain areas and number of rain days decreased over the urban area of Beijing, whereas the mean rain areas decreased but the number of
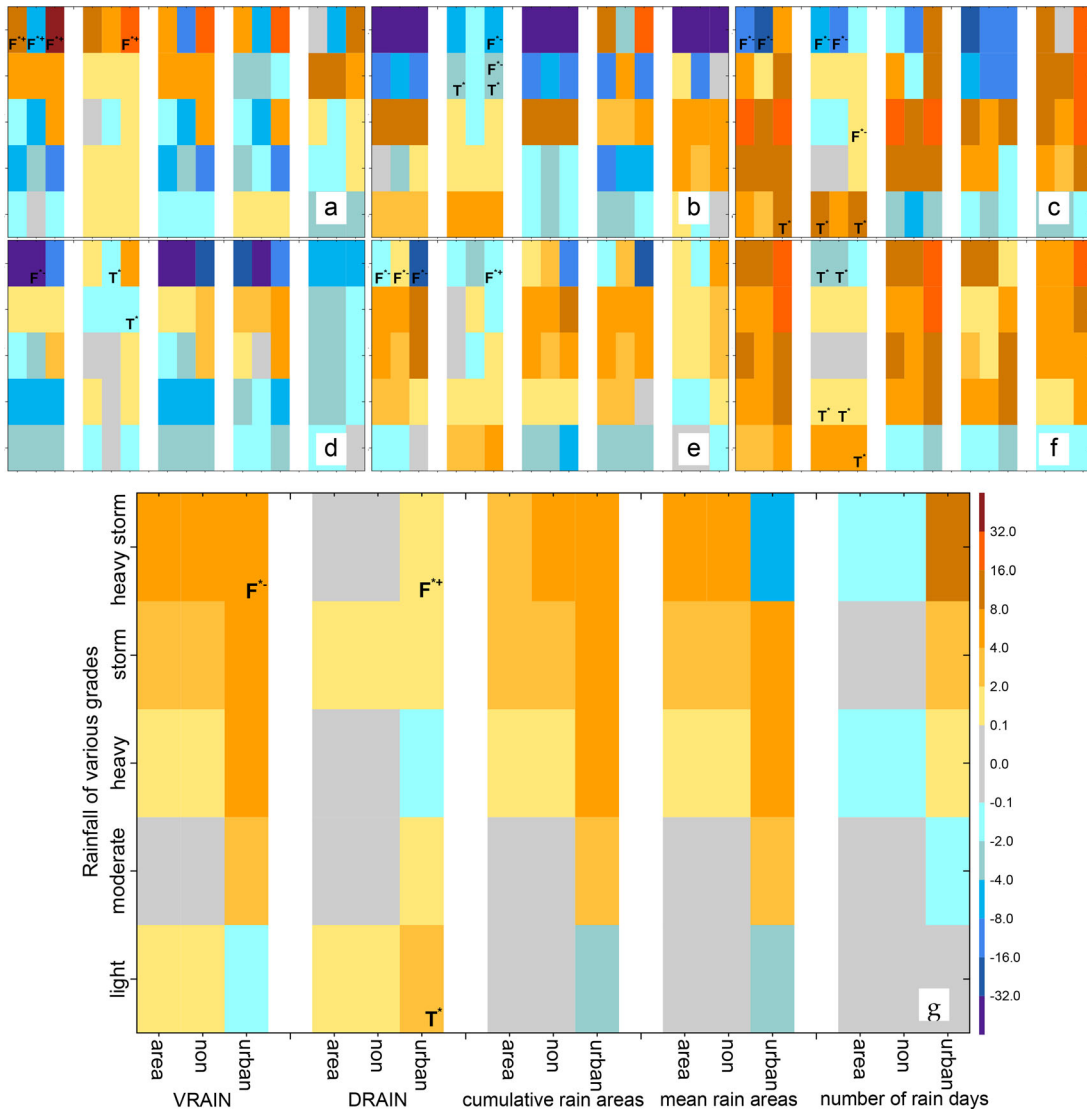
*Fig. 2.*    The urban-induced relative changes in rainfall of various intensity levels at different spatial scales. Changes in VRAIN, DRAIN, cumulative rain areas, mean rain areas, and numbers of rain days for various intensity levels of rainfall over nonurban areas (non), urban areas, and subregions as a whole (a: Beijing, b: Shanghai, c: Guangzhou, d: BTH, e: YRD, f: PRD, g: China) due to urban surface expansion between 1980 and 2010 (units: %).

rain days remained similar over the urban areas of China as a whole. The urban-induced changes in total rainfall in terms of both variability and intensity between areas defined as urban surfaces under both U80 and U10 (U2U) and U10 only (N2U) exhibited marked sub-regional characteristics for VRAIN and DRAIN (Fig. S3, see Supplemental Online Material: text S1).

### 3.2. Urban-induced changes in rainfall at various intensity levels

The urban-induced relative changes in rainfall of various intensity levels over Beijing revealed significantly enhanced variability in DRAIN and VRAIN for heavy storm rain only (Fig. 2a and Supplemental Online Material Table S1). Both the variability in DRAIN and VRAIN tended to increase over urban areas, whereas only the variability of VRAIN increased over nonurban areas (although VRAIN intensity decreased) and the entirety of Beijing. The increased VRAIN over urban areas (42.8%$^{F*}$) and slightly decreased VRAIN over non-urban areas (–4.5%$^{F*}$) resulted in increased VRAIN over the whole of Beijing (14.2%$^{F*}$). The increased VRAIN over urban areas (42.8%$^{F*}$) could be attributed to increased DRAIN (19.0%$^{F*}$) and greater cumulative rain areas (29.3%) due to increased mean rain areas (22.5%)

and number of rain days (8.8%). However, over nonurban areas, increased DRAIN (6.0%) and decreased cumulative rain areas (–11.1%) due to decreased mean rain areas (–5.5%) and number of rain days (–5.4%) contributed to reduced VRAIN (–4.5%$^{F*}$), showing that the contributions to VRAIN changes from the decreased mean rain areas and number of rain days were larger than those from the increased DRAIN. Overall, increased DRAIN (10.3%) and greater cumulative rain areas (4.4%), due to the increased mean rain areas only, contributed to increased VRAIN (14.2%$^{F*}$) over Beijing as a whole.

The urban-induced changes in rainfall over Shanghai revealed significantly weakened DRAIN variability and intensity only for storm and heavy storm rain (Fig. 2b and Supplemental Online Material Table S1). For heavy storm rain, DRAIN variability decreased over urban areas, for which changes in both DRAIN (–7.7%$^{F*}$) and cumulative rain areas (–46.8%) contributed to decreased VRAIN (–58.1%). The changes in mean rain areas (19.0%) and number of rain days (–81.3%) were opposite, and the change in the number of rain days made a greater contribution to VRAIN change than did the change in mean rain areas. For storm rain, DRAIN variability and intensity both decreased over urban areas, whereas only DRAIN intensity decreased over Shanghai as a whole. Changes in both DRAIN (–2.5%$^{F*T*}$ and –2.3%$^{T*}$) and cumulative rain areas (–12.1% and –11.7%) contributed to the weakened VRAIN (–14.8% and –14.2%) over the urban and entire areas of Shanghai. The decreased cumulative rain areas could be attributed to decreased mean rain areas (–12.1%) only over urban areas, whereas the changes in mean rain areas (–13.7%) and number of rain days (1.8%) were opposite over the entirety of Shanghai, showing that the influence of the mean rain areas on VRAIN and cumulative rain areas was larger than that of the number of rain days.

The urban-induced changes in rainfall over Guangzhou indicated significant DRAIN and VRAIN variability for heavy and heavy storm rain and DRAIN and VRAIN intensity for light rain (Fig. 2c and Supplemental Online Material Table S1). For heavy storm rain, DRAIN and VRAIN variability decreased over nonurban areas and the entirety of Guangzhou. Changes in both DRAIN (–12.5%$^{F*}$ and –7.5%$^{F*}$) and cumulative rain areas (–10.5% and –1.9%) contributed to decreased VRAIN (–24.3%$^{F*}$ and –9.5%$^{F*}$). Changes in cumulative rain areas could be attributed to changes in mean rain areas (–10.5%) only over nonurban areas, whereas the changes in mean rain areas (−17.7%) and number of rain days (13.4%) were opposite over the entirety of Guangzhou, showing that the influence of the mean rain areas on VRAIN was larger than that of the number of rain days.

For heavy rain, DRAIN variability decreased over urban areas, whereas DRAIN intensity increased. Changes in both mean rain areas (9.0%) and number of rain days (16.8%) contributed to increased cumulative rain areas (24.2%), and DRAIN (0.6%$^{F*}$) induced an increase in VRAIN (24.7%) over urban areas. For light rain, DRAIN/VRAIN intensity increased over urban areas and only DRAIN intensity increased over the entirety of Guangzhou. Changes in both mean rain areas (–1.4% and –1.7%) and number of rain days (–1.2% and –2.3%) contributed to the decreased cumulative rain areas (–2.6% and –4.0%) over the urban and entire areas of Guangzhou. The intensified DRAIN (11.5%$^{T*}$/9.3%$^{T*}$) induced an increase in VRAIN (9.2%$^{T*}$ and 5.6%), showing that the higher DRAIN made a greater contribution to VRAIN changes than did the cumulative rain areas.

The urban-induced changes in rainfall over BTH revealed significantly weakened DRAIN intensity and VRAIN variability over nonurban areas for heavy storm rain, as well as decreased DRAIN intensity over urban areas for storm rain (Fig. 2d and Supplemental Online Material Table S1). For heavy storm rain, changes in both mean rain areas (–33.8%) and number of rain days (–4.1%) contributed to decreased cumulative rain areas (–39.2%), and the weakened DRAIN (–0.7%$^{T*}$) led to a weakened VRAIN (–40.2%$^{F*}$) over nonurban areas. For storm rain, the decreased DRAIN (–1.7%$^{T*}$) and increased cumulative rain areas (3.5%), due to greater mean rain areas (4.2%) and reduced number of rain days (–0.7%), resulted in an increased VRAIN (1.9%) over urban areas, showing that the mean rain areas made a greater contribution to VRAIN changes than did the decreased DRAIN and number of rain days.

The urban-induced changes in rainfall over the YRD revealed significant changes for heavy storm rain only, showing increased DRAIN variability over urban areas (although DRAIN intensity decreased) and decreased VRAIN variability over nonurban areas (although VRAIN intensity increased), urban areas, and the entirety of YRD (Fig. 2e and Supplemental Online Material Table S1). DRAIN decreased over urban areas only, although the decreased VRAIN over urban areas (–16.7%$^{F*}$) combined with the slightly increased VRAIN over nonurban areas (1.1%$^{F*}$) resulted in a decreased VRAIN over the entirety of YRD (–1.4%$^{F*}$). Changes in both DRAIN (–0.7%$^{F*}$) and cumulative rain areas (–15.9%) contributed to the decreased VRAIN (–16.7%$^{F*}$) over urban areas. The changes in mean rain areas (–22.2%) and number of rain days (5.1%) were opposite, showing that the mean rain areas had a greater impact on the cumulative rain areas than did the number of rain days. However, the increased cumulative rain areas (3.3%) and weakened DRAIN (–2.2%) led to an

increased VRAIN over nonurban areas ($1.1\%^{F*}$). The changes in mean rain areas (3.8%) and number of rain days (–0.5%) were opposite, showing that (i) the change in cumulative rain areas had a greater impact on the VRAIN and cumulative rain areas than did the change in DRAIN and (ii) the mean rain areas had a larger influence on the cumulative rain areas than did the number of rain days. Overall, the increased cumulative rain areas (0.5%) but decreased DRAIN (–1.9%) led to a decreased VRAIN ($–1.4\%^{F*}$) over the entire YRD. The changes in mean rain areas (–0.7%) and number of rain days (1.2%) were opposite, showing that (i) DRAIN had a greater impact on VRAIN than did the change in cumulative rain areas and (ii) the number of rain days had a larger influence on the cumulative rain areas than did the mean rain areas.

The urban-induced changes in rainfall over the PRD indicated significant changes in DRAIN only, showing decreased DRAIN intensity over nonurban areas and the entirety of the PRD for heavy storm rain and increased DRAIN intensity over nonurban areas and the entirety of the PRD for moderate rain and over urban areas for light rain (Fig. 2f and Supplemental Online Material Table S1). For heavy storm rain, the decreased DRAIN ($–2.9\%^{T*}$ and $–2.6\%^{T*}$) and increased cumulative rain areas (13.8% and 14.7%) led to increased VRAIN (11.3% and 12.4%) over the nonurban and entire areas of the PRD. Changes in both the mean rain areas (10.2% and 9.9%) and number of rain days (4.1% and 5.3%) contributed to increased cumulative rain areas, showing that the changes in the cumulative rain areas had a greater impact on VRAIN cumulative rain areas than did the changes in DRAIN. For moderate rain, changes in mean rain areas (4.9% and 5.9%) and number of rain days (1.5% and 1.5%) both contributed to increased cumulative rain areas (6.3% and 7.2%) over the nonurban and entire areas of the PRD, with which the intensified DRAIN ($0.3\%^{T*}$ and $0.3\%^{T*}$) resulted in increased VRAIN (6.5% and 7.5%). For light rain, the increased DRAIN ($7.4\%^{T*}$) and decreased cumulative rain areas (–2.7%) led to increased VRAIN (4.9%) over urban areas. Changes in mean rain areas (–2.1%) and number of rain days (–0.6%) both contributed to the decreased cumulative rain areas, showing that the increased DRAIN had a greater impact on VRAIN than did the decreased cumulative rain areas.

The urban-induced changes in rainfall over China as a whole revealed significant changes over urban areas only, showing increased DRAIN variability and decreased VRAIN variability for heavy storm rain and increased DRAIN intensity only for light rain (Fig. 2g and Supplemental Online Material Table S1). For heavy storm rain, changes in DRAIN ($1.6\%^{F*}$) and cumulative rain areas (6.0%) both contributed to the increased VRAIN ($7.5\%^{F*}$). The changes in the mean rain areas (–8.0%) and number of rain days (13.0%) were opposite, indicating that the increased number of rain days had a larger impact on the cumulative rain areas than did the decreased mean rain areas. For light rain, the increased DRAIN ($3.2\%^{T*}$) and decreased cumulative rain areas (–3.4%) resulted in a decrease in VRAIN (–0.2%). Changes in the mean rain areas (–3.4%) were responsible for the changes in cumulative rain areas with the number of rain days unchanged.

The urban-induced changes in rainfall of various intensity levels in terms of both variability and intensity between U2U and N2U also exhibited marked subregional characteristics for VRAIN and DRAIN (see Supplemental Online Material Fig. S4: text S2).

In sum, the risk of heavy storm rain increased owing to an increase in the variability in DRAIN and VRAIN over urban areas, nonurban areas, the entirety of Beijing, and over urban areas of the YRD and all of China. Both the variability in DRAIN and VRAIN increased over urban areas of Beijing, for which the mean rain areas and number of rain days increased. By contrast, only the variability in VRAIN increased over nonurban areas (although its intensity decreased) and the entirety of Beijing, for which both the mean rain areas and number of rain days decreased over the nonurban areas of Beijing and only the mean rain areas increased over Beijing as a whole. The variability in DRAIN increased while that in VRAIN decreased over the urban areas of the YRD (although the intensity of DRAIN decreased) and China as a whole (although the intensity of VRAIN increased). The reduced mean rain areas and increased number of rain days resulted in reduced cumulative rain areas over the urban areas of the YRD, but increased over urban areas of China as a whole.

The risk of heavy storm rain decreased owing to reduced variability in DRAIN and VRAIN, and a reduction in the intensities of DRAIN over urban areas of Shanghai, nonurban areas of BTH, and nonurban and all areas of Guangzhou, the YRD, and the PRD. Only the variability in DRAIN decreased over the urban areas of Shanghai, for which the increase in the mean rain areas and decrease in the number of rain days led to decreased variability in VRAIN (but not significant). The variability in DRAIN and VRAIN decreased over nonurban areas and the entirety of Guangzhou owing to decreased cumulative rain areas. In these subregions, the mean rain areas decreased and number of rain days increased over Guangzhou as a whole, whereas only the mean rain areas decreased over nonurban areas of Guangzhou. Both variability in VRAIN and intensity in DRAIN decreased over the nonurban areas of BTH, for which both the mean rain areas and number of rain days decreased.

Although changes in DRAIN were not significant, the variability in VRAIN decreased over nonurban areas (although rainfall intensity in VRAIN increased) and the entirety of the YRD. For these subregions, the mean rain areas increased and the number of rain days decreased over nonurban areas, whereas the mean rain areas decreased and the number of rain days increased over the entire YRD. Only the intensity of DRAIN decreased over the nonurban areas and the entire PRD, for which the increased mean rain areas and number of rain days led to an increase in VRAIN (but not significant).

### 3.3. Changes in probability of VRAIN and DRAIN for heavy storm rain

The probability distributions of different DRAIN and VRAIN (the natural logarithms of VRAIN were used to more clearly present the results, owing to the wide range of VRAIN) over urban areas, nonurban areas, and the entirety of Beijing for urban surface expansion from 1980 to 2010 are shown in Fig. 3.

The probability of DRAIN generally increased for smaller and larger values, especially for values exceeding 150 mm day$^{-1}$ over urban areas of Beijing, which led to a wider variability in DRAIN and an increase in the intensity in DRAIN by 19.0%. The computed $F_{U10/U80}$ values (the values under U10 divided by that under U80) were 1.1 and 5.4 over nonurban areas and urban areas, which resulted in 1.3 for $F_{U10/U80}$ value over entirety of Beijing. $F_{U10/U80}$ values were detected to be larger over urban areas, showing enhanced DRAIN variability over urban areas only. The corresponding probability of VRAIN also displayed marked differences between U80 and U10 over not only urban areas but also over nonurban areas and the entirety of Beijing, which led to increased VRAIN variability, showing an increase in VRAIN of 42.8% over urban areas while a decrease of –4.5% over nonurban areas, which resulted in an increase of VRAIN by 14.2% over the entirety of Beijing. The $F_{U10/U80}$ values were 1.8 and 2.7 over nonurban areas and urban areas, and resulted in a $F_{U10/U80}$ value of 2.7 over entirety of Beijing, showing enhanced VRAIN variability over different subregions with the larger value over urban areas than that over nonurban areas.

### 3.4. Changes in percentages and absolute values of VRAIN at various intensity levels

The percentages and absolute values of VRAIN for various intensity levels of rainfall over different subregions under U80 and U10 are presented in Figs. 4 and 5. The percentage differences in VRAIN between U80 and U10 (Fig. 4) were generally consistent with the changes shown

in Fig. 2, with the exception of some subregions, which can be attributed to urban-induced changes in the VRAIN for rainfalls at various levels of intensity and the accumulated VRAIN (Fig. 5).

The values of VRAIN for heavy storm rain and the corresponding percentage relative to the total amount of rainfall were small and generally less than 5% over Beijing, Shanghai, BTH, the YRD, and China as a whole and less than 10% over Guangzhou and the PRD, which can be attributed to smaller mean rain areas and fewer numbers of rain days for heavy storm rain, compared with rainfall at other levels of intensity. Taking Beijing as an example, the annual mean number of rain days for heavy storm rain might have been several days, whereas the corresponding number for moderate rain were 20 times higher. However, heavy storm rain had a severe impact on daily life (Meng et al., 2013). Therefore, the influence of heavy storm rain on hydrological applications and management warrants substantial attention, despite the fact that the absolute values of VRAIN and their percentages relative to the total amount of rainfall were small.

Although the percentage of VRAIN for heavy storm rain decreased, the magnitude increased. As an example, for a heavy storm rain over Guangzhou, the percentages of VRAIN consistently decreased over nonurban areas, urban areas, and the entirety of Guangzhou; however, the corresponding absolute values of VRAIN increased over urban areas, but decreased over nonurban areas and the entirety of Guangzhou. These differences can be interpreted by the differences of changes in the VRAIN between U80 and U10 for heavy storm rain and the accumulated. The accumulated VRAIN increased by 4.0%, 15.4%, and 9.2% over nonurban areas, urban areas, and the entirety of Guangzhou, respectively, larger than those for the heavy storm rain (–24.3%, 7.7%, and –9.5%).

### 3.5. Physical mechanism of changes in rainfall

Rainfall is controlled mainly by the development of vertical motions of the air and the water vapour supply. Changes in DRAIN and VRAIN for total rainfall and rainfall at various intensity levels could be interpreted by urban-induced changes in the vertical velocity and moisture flux. Changes in the water vapour supply could be divided into two aspects, namely (i) the local moisture flux from the surface evaporation and (ii) the moisture flux connected with large-scale circulation transport, namely water vapour transport related to the East Asian summer monsoon (EASM).

With the urban surface expansion between U80 and U10, especially for surfaces converted from nonurban to urban ones, the annual mean vertical motions were
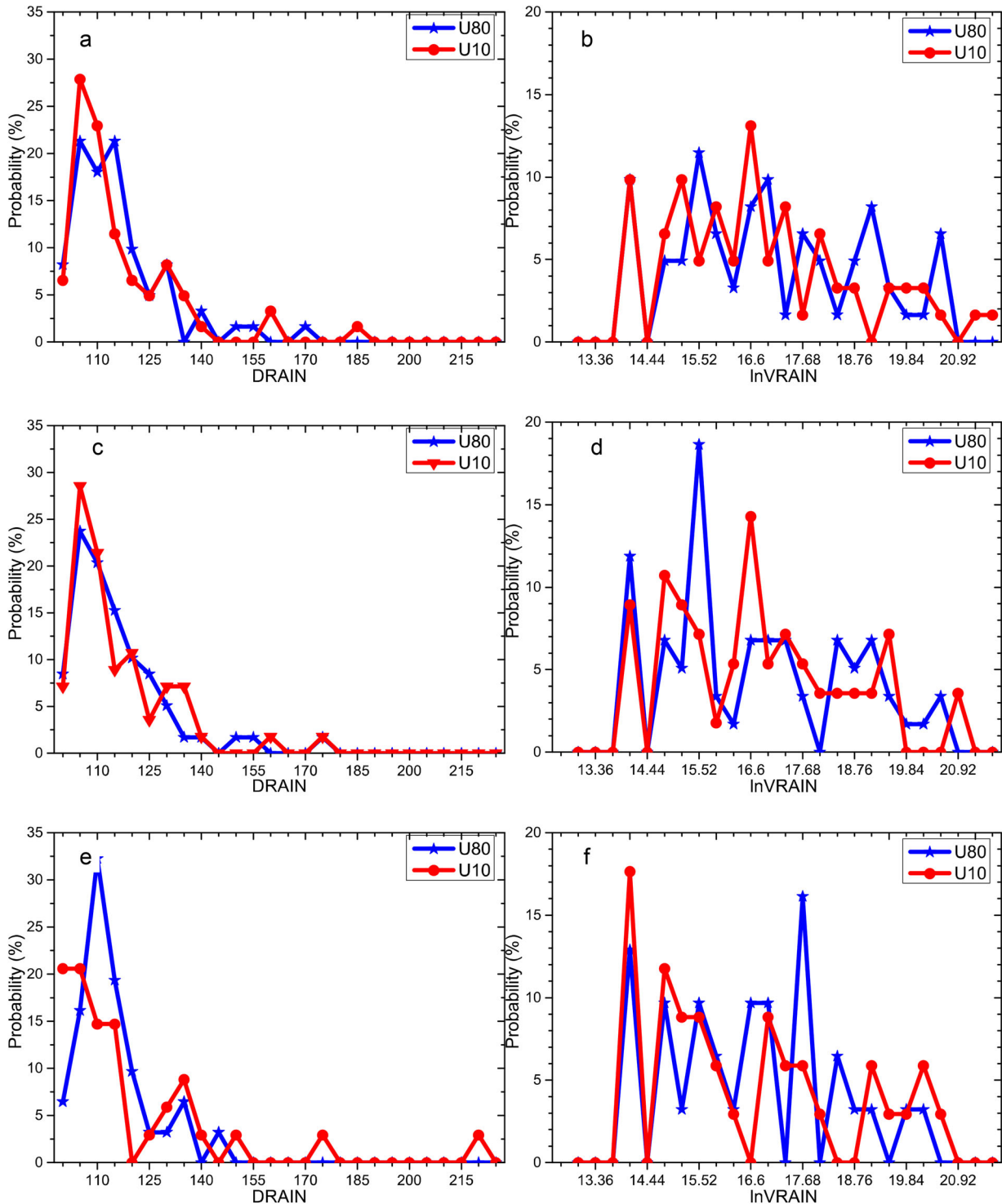
Fig. 3. Probability distributions of different (a, c, e, units: mm day$^{-1}$) DRAIN and (b, d, f, units: m$^3$) lnVRAIN for heavy storm rain over (c, d) nonurban areas, (e, f) urban areas, and (a, b) the entirety of Beijing due to urban surface expansion between 1980 and 2010.

strengthened over three cities [Beijing (39.9°N, 116.3°E), Shanghai (31.14°N, 121.29°E), and Guangzhou (23.08°N, 113.14°E)] and three city clusters (the BTH, YRD, and

PRD) because of the urban heat island effect (Fig. 6). However, changes in total rainfall and rainfall at various intensity levels expressed marked subregional
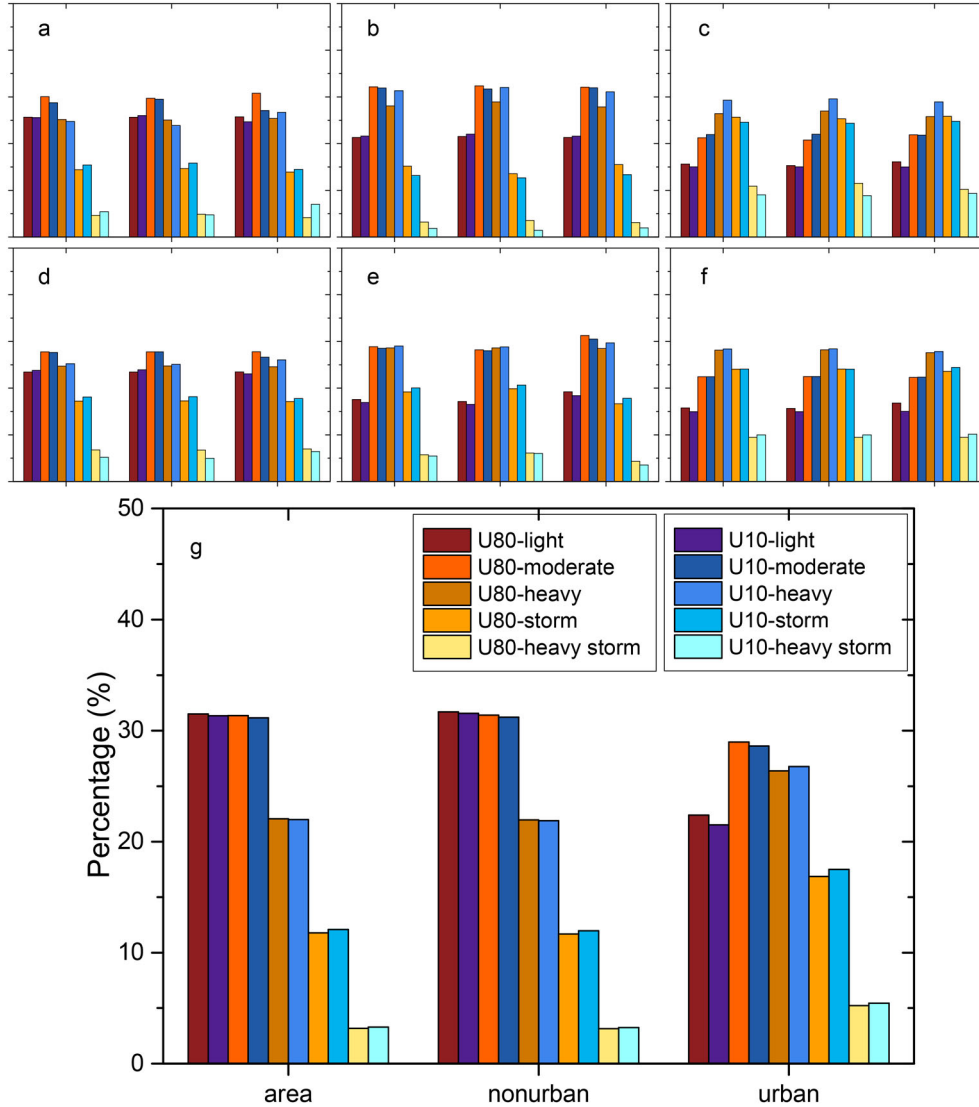
*Fig. 4.* Percentages of VRAIN for various intensity levels of rainfall over different subregions (a: Beijing, b: Shanghai, c: Guangzhou, d: BTH, e: YRD, f: PRD, g: China) under U80 and U10.

characteristics, which can be explained by changes in the moisture flux due to urban surface expansion.

The increased use of impervious surfaces in urban areas affected the sensible and latent heat fluxes, resulting in changes in energy and water exchanges between the land and the atmosphere (Zhao and Wu, 2017). However, changes in sensible and latent heat fluxes over nonurban areas were generally opposite to those over urban areas. In total, changes in the sensible and latent heat fluxes over the entire areas of the three cities and three city clusters were generally consistent with those over urban areas. The local upward moisture generally decreased over the entirety of the three cities and three city clusters, especially over the urban areas.

The rainfall in the EAM region is primarily concentrated during summer time because of a typical monsoon characteristic over the studied domain. Meanwhile, significant changes in DRAIN and VRAIN for rainfall at various intensity levels were detected mainly for storm rainfall and heavy storm rainfall, which mostly occurred in the EASM periods. Therefore, urban-induced changes in EASM-related moisture flux are to be explored. With the urban surface expansion between U80 and U10, the southwesterly currents from the Bay of Bengal and southeasterly currents from the subtropical high in the northwestern Pacific weakened, whereas the southerly currents from the South China Sea and the westerly currents at middle–high latitudes strengthened (Zhao and Wu, 2017,
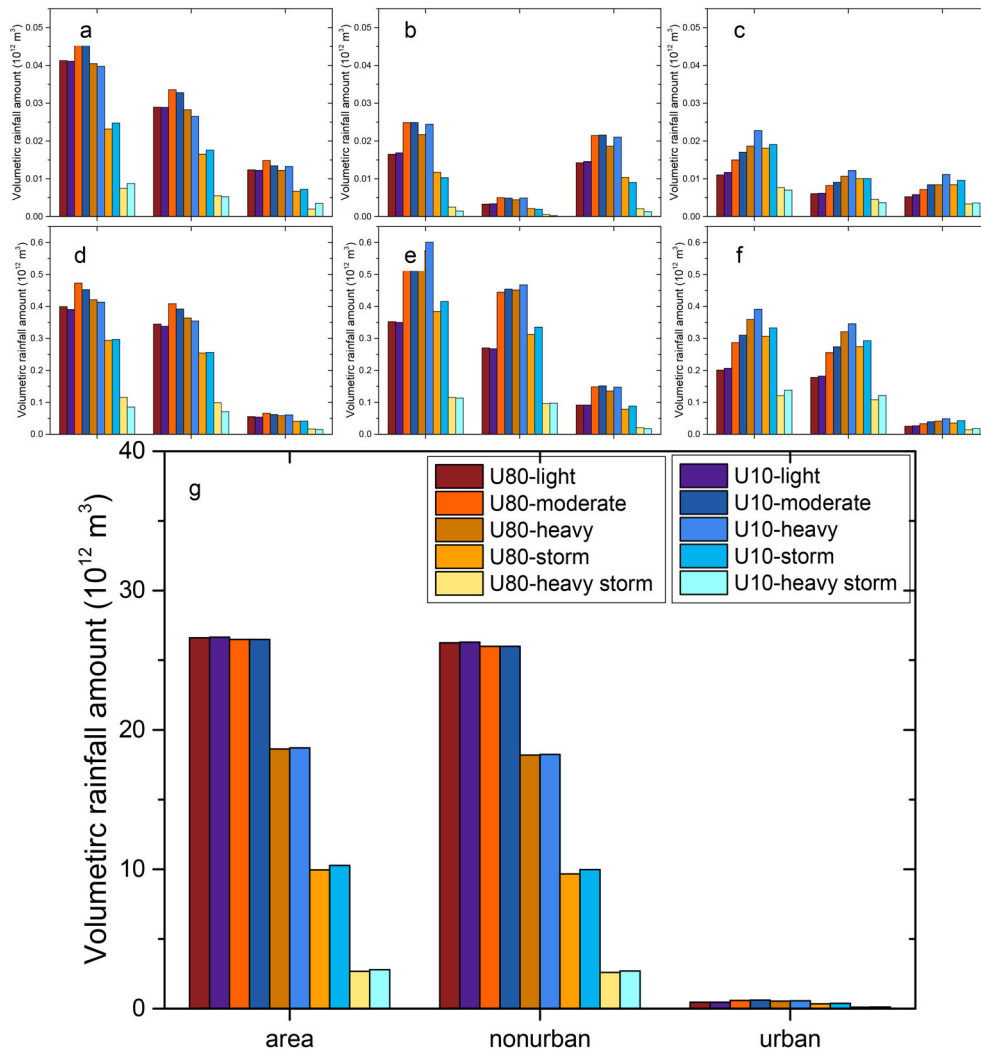
Fig. 5. VRAIN for various intensity levels of rainfall over different subregions (a: Beijing, b: Shanghai, c: Guangzhou, d: BTH, e: YRD, f: PRD, g: China) under U80 and U10.

see Supplemental Online Material Fig. S5: text S3). Furthermore, the influenced EASM-related currents affected the subregional water vapour supply over the three cities and three city clusters.

*3.5.1. Causes of changes in total rainfall.* At city-cluster scales, the annual precipitable water decreased over the BTH, but increased over the YRD and PRD (Fig. 7a–c and Supplemental Online Material Table S2). Changes in the values of DRAIN for total rainfall were consistent with those of precipitable water, whereas significant changes in total rainfall passing 95% *t* tests were detected only over urban areas of the PRD (Fig. 1), showing the aforementioned an increase in the intensity. The decreased rainfall frequency and increased mean rain

areas contributed to the increased intensity of VRAIN over urban areas of the PRD.

At city scales, changes in DRAIN for the total rainfall over subregions of Guangzhou and Shanghai were similar to those over the PRD and YRD, respectively. However, changes in DRAIN over urban areas and the entirety of Beijing were different with those over the corresponding subregions of the BTH (Fig. 1). Changes in annual averaged precipitable water at city scales were quite similar to those at city-cluster scales (Supplemental Online Material Table S2). The inconsistency between changes in DRAIN and those of the precipitable water between the cities and city clusters might be interpreted as changes in annual water vapour mixing ratio. Pressure longitudinal and latitudinal cross-sections displaying changes in the annual
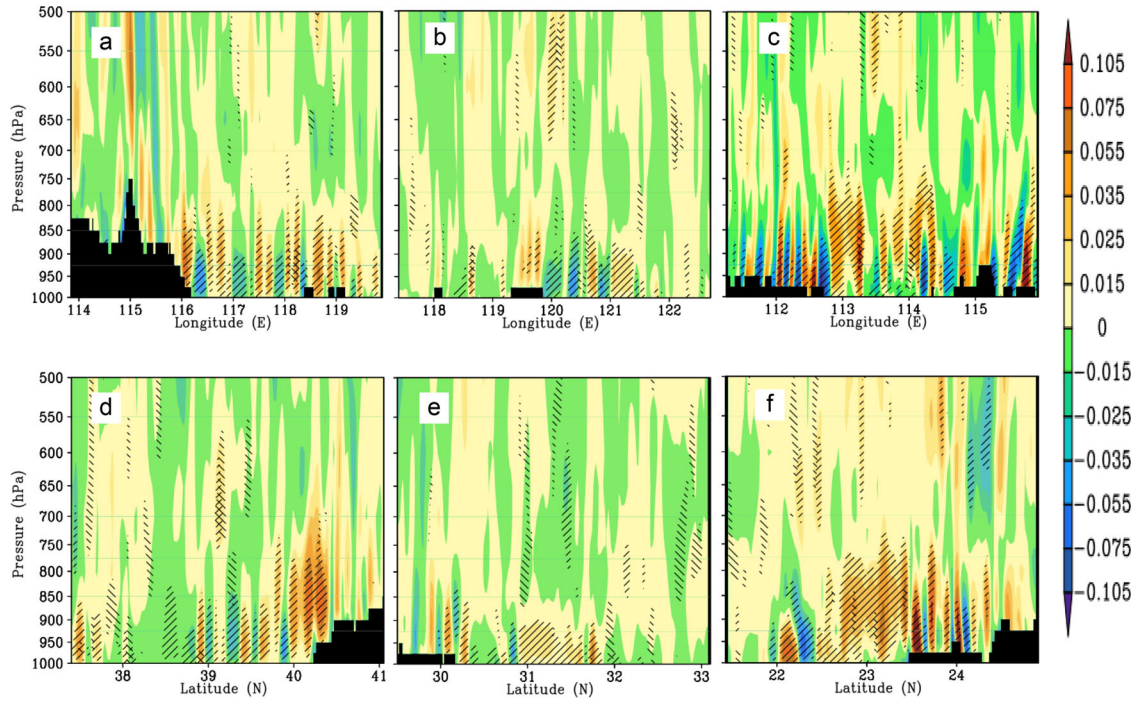
*Fig. 6.* Pressure (a–c) longitudinal and (d–f) latitudinal cross-sections along the (a) 39.9°N, (b) 31.14°N, (c) 23.08°N and (d) 116.3°E, (e) 121.29°E, (f) 113.14°E axes (black areas for topography) showing changes in the vertical velocity (shaded) in annual from U10 to U80 over the three city clusters of the (a, d) BTH, (b, e) YRD and (c, f) PRD at 3.3-km resolution [units: $10^{-1}$ m s$^{-1}$, slashes ( / ) and backslashes (\) denote areas that are significant at the 95% confidence level *t* tests and *F* tests].
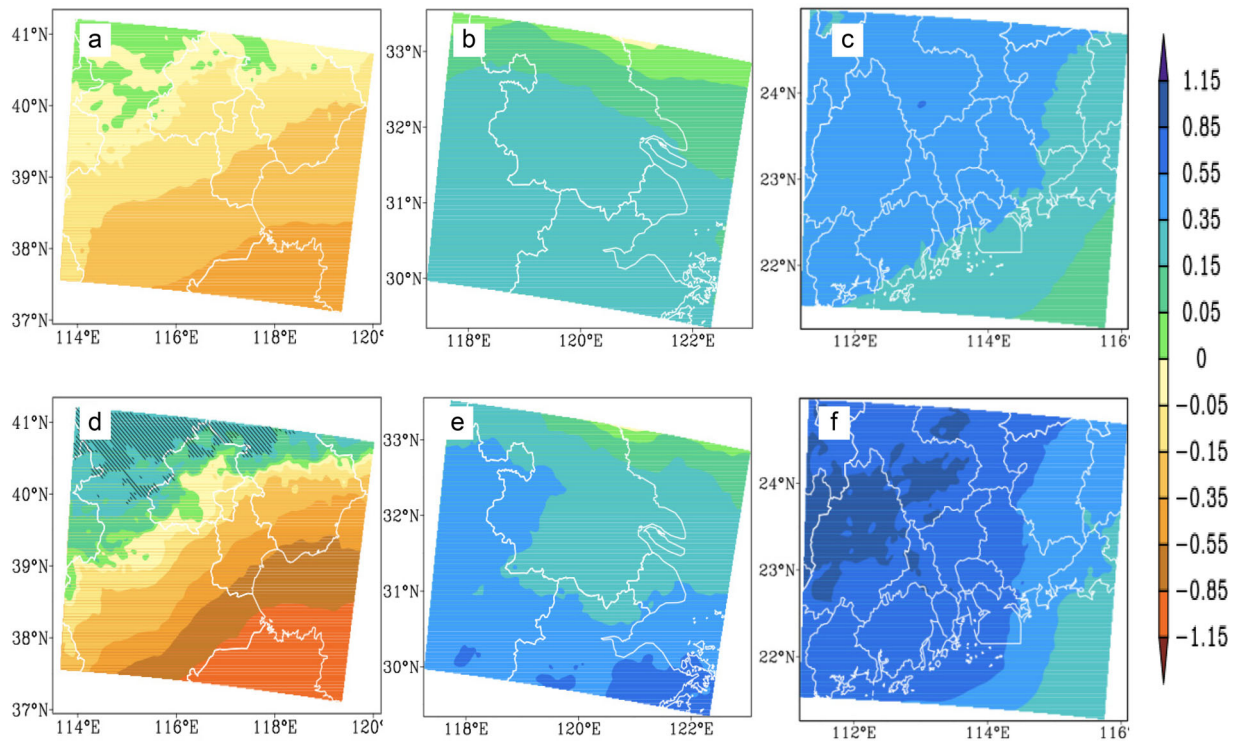


*Fig. 7.* Changes in (a–c) annual and (d–f) summer precipitable water from U10 to U80 over the three city clusters of the (a, d) BTH, (b, e) YRD, and (c, f) PRD at a 3.3 km resolution (units: mm, white curves for geographic boundaries).
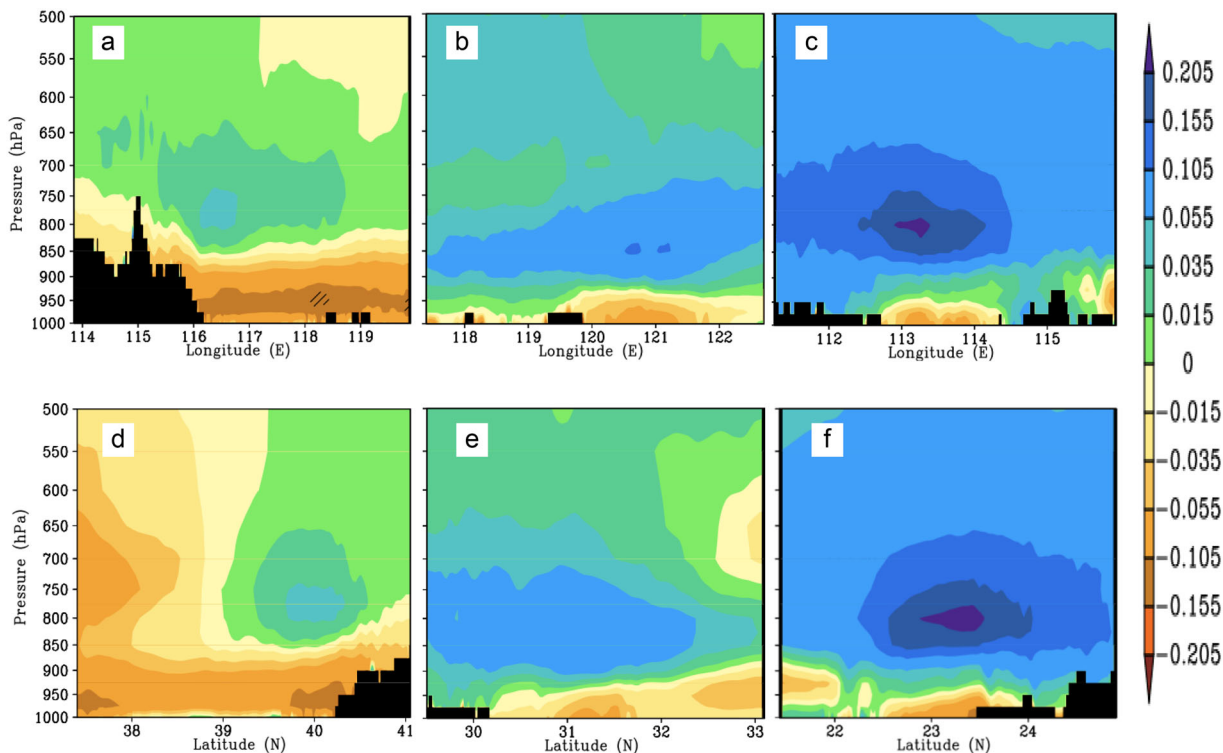
*Fig. 8.* Pressure (a–c) longitudinal and (d–f) latitudinal cross-sections along the (a) 39.9°N, (b) 31.14°N, (c) 23.08°N and (d) 116.3°E, (e) 121.29°E, (f) 113.14°E axes (black areas for topography) showing changes in the water vapour mixing ratio (shaded) in annual from U10 to U80 over the three city clusters of the (a, d) BTH, (b, e) YRD, and (c, f) PRD at 3.3-km resolution (units: $10^{-3}$ kg kg$^{-1}$).

water vapour mixing ratio from U10 to U80 over the three city clusters of the BTH, YRD, and PRD are shown in Fig. 8. There was drying tendency for the water vapour mixing ratio in the lower troposphere but a wetting tendency in the low–middle troposphere due to urban surface expansion over the BTH, YRD, and PRD with the exception of the decreasing water vapour mixing ratio over the BTH. However, high centres for changes in the water vapour mixing ratio were found over the three cities.

Consequently, although the water vapour mixing ratio turned to dry in the lower troposphere over the three cities, the enhanced water vapour mixing ratio in the low–middle troposphere and the enhanced vertical velocity resulted in the increased DRAIN for the total rainfall, which was significant over urban areas of Beijing and Guangzhou, showing enhanced variability for the former and increased intensity for the latter. The decreased rainfall frequency and mean rain areas contributed to the enhanced variability for VRAIN over urban areas of Beijing, whereas, the decreased rainfall frequency and increased mean rain areas contributed to the increased intensity for VRAIN over urban areas of Guangzhou.

Overall, changes in both DRAIN and VRAIN displayed increased intensity over the entirety of China. However, only the changes in DRAIN were significant.

*3.5.2. Causes of changes in rainfall at various intensity levels.* Changes in DRAIN and VRAIN were found to be more pronounced for storm and heavy storm rain, which occurred mainly in summer. To concentrate our analysis more directly on storm rain and heavy storm rain, we explore in detail the changes in DRAIN and VRAIN in summer alone.

*3.5.2.1. Over the BTH and Beijing.* Urban-induced changes in rainfall at various intensity levels in the summer displayed significant changes in DRAIN and VRAIN for both storm rain and heavy storm rain only over the BTH, but for heavy storm rain only over Beijing.

Over the BTH, the EASM-related moisture flux expressed the westerly or southwesterly currents, which were larger in the eastern part and smaller in the western part (Fig. 9a). Urban-induced changes in moisture flux displayed the weakened southwesterly currents in the eastern part but the enhanced westerly currents in the
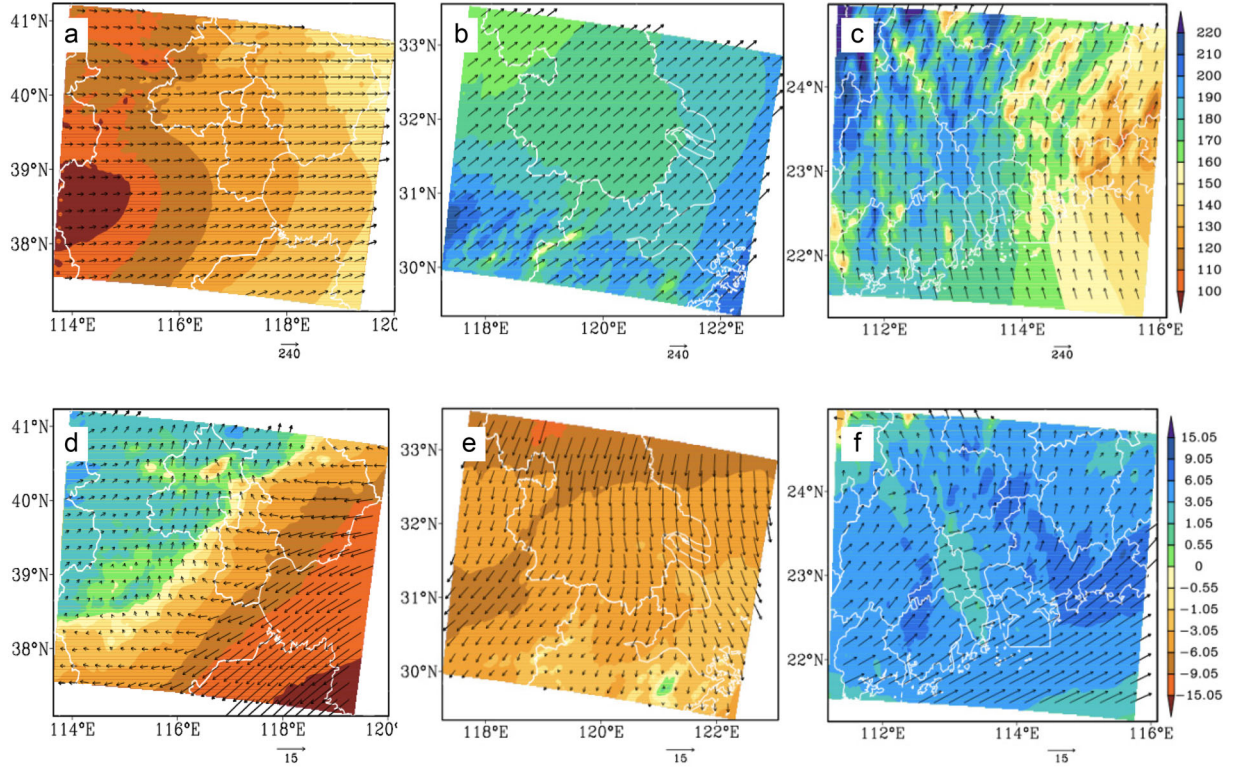
*Fig. 9.* Spatial distributions of (a–c) mean moisture flux (shaded) and vectors for U80, and (d–f) the corresponding changes from U10 to U80 across the whole troposphere in the summer over the three city clusters of the (a, d) BTH, (b, e) YRD, and (c, f) PRD at 3.3-km resolution (units: $10^{-3}$ kg m$^{-1}$ s$^{-1}$, white curves for geographic boundaries].

western part (Fig. 9d), which induced the increased precipitable water in the northwestern part but decreased in the southeastern part (Fig. 7d). Overall, the decreased local moisture flux and the generally weakened EASM-related water vapour transport resulted in a decrease in the precipitable water over the BTH, which resulted in a decrease in DRAIN over urban areas for storm rain and nonurban areas for heavy storm rain, although the vertical motions strengthened (Fig. 10a and d). Meanwhile, the decreased DRAIN intensity, accompanied by the decreased rainfall frequency and mean areas, resulted in the weakened VRAIN variability for heavy storm rain over nonurban areas.

Over Beijing, changes in the EASM-related water vapour transport were positive (Fig. 9d), showing the enhanced westerly currents, which resulted in increased precipitable water (Fig. 7d). The moisture flux over Beijing decreased in the lower troposphere but increased in the low–middle troposphere (Fig. 11a and d), which could be attributed to the changes in the wind speeds (Fig. 12a and d) and water vapour mixing ratio (Fig. 13a and d). Therefore, the enhanced vertical motions (Fig. 10a and d), the decreased latent heat flux (Supplemental Online Material Table S2), and the enhanced EASM-

related moisture flux helped to increase the rainfall at various intensity levels over Beijing. However, the enhanced vertical motions and the wetting tendency in the low–middle troposphere and the drying tendency in the lower troposphere helped in the development of a deep convective system, resulting in significant changes in DRAIN for heavy storm rain only over urban areas. Changes in VRAIN for heavy storm rain were all significant over urban and nonurban areas and the entirety of Beijing because of the corresponding changes in rainfall frequency and mean rain areas, showing the intensified VRAIN variability.

Heavy storm rain over Beijing was highly affected by the EASM-related circulation and moisture flux. Previous studies have demonstrated the importance of enhanced vertical velocity and adequate moisture flux, as well as stable synoptic systems, such as the development and maintenance of the Hetao cyclone, Huanghuai cyclone, etc., whose restrained eastward or northward movements helped in the occurrence and duration of heavy storm rain (Meng et al., 2013). The decreased water vapour mixing ratio in the lower troposphere, the increased VRAIN and DRAIN variability over Beijing could be interpreted as the convergence of the enhanced westerly-
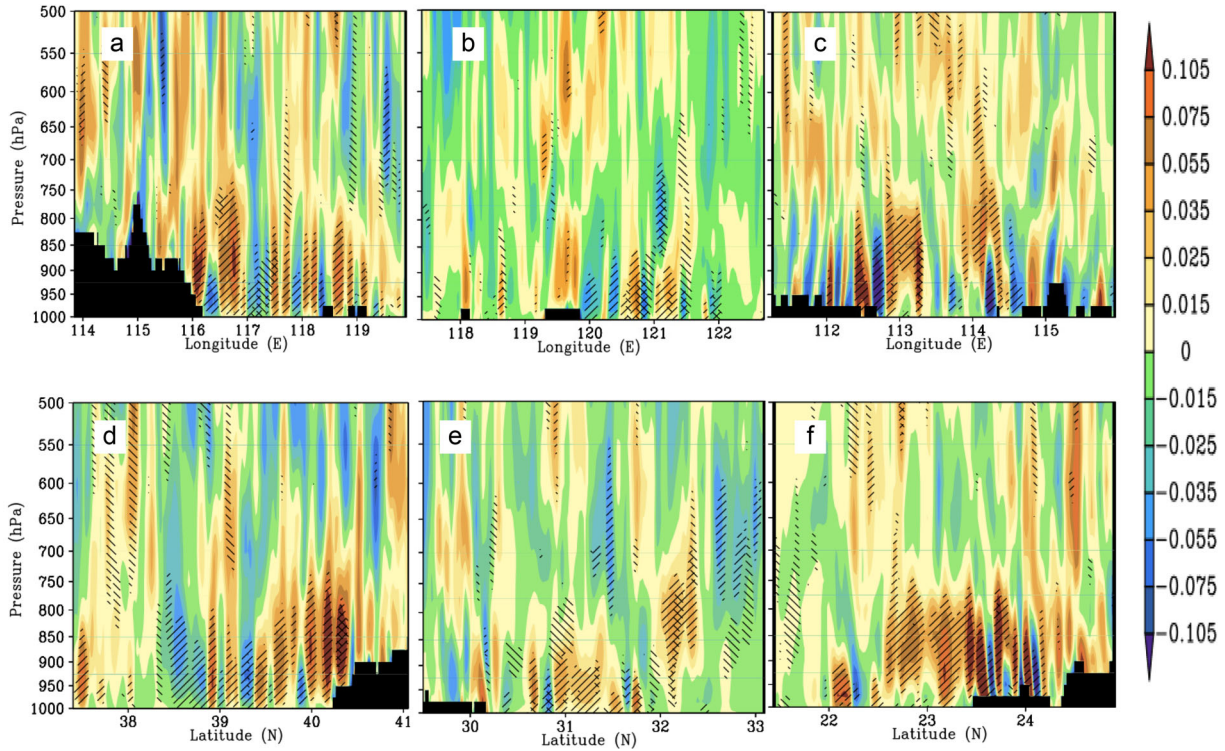
Fig. 10.    Same as Fig. 6, bit for the results in the summer.

related cold air mass and decreased northward monsoon circulation-related warm air mass over the northern part of China, which helped in the development and maintenance of severe weather systems while restraining the northward or eastward movement of these systems, under the combined influence of urban-induced strengthened vertical velocity.

*3.5.2.2. Over the YRD and Shanghai.* Urban-induced changes in rainfall at various intensity levels in the summer displayed significant changes for heavy storm rain only over the YRD and for storm rain and heavy storm rain over Shanghai.

The EASM-related moisture flux expressed the southwesterly currents across the whole troposphere (Fig. 9b), for which urban-induced changes displayed the weakened southwesterly currents (Fig. 9e). However, the precipitable water in the summer increased across the entire areas (Fig. 7e). The differences between the weakened EASM-related moisture flux and the increased precipitable water could be interpreted by the decreased wind speeds from the lower to middle troposphere (Fig. 12b and e), and by the drying tendency in the lower troposphere and wetting tendency in the low–middle troposphere for the water vapour mixing ratio (Fig. 13b and e). The decreased moisture flux could be attributed mainly to the decreased wind speeds, whereas the increased precipitable water

could be attributed mainly to the increased water vapour mixing ratio, which resulted in a large decrease in EASM-related moisture flux in the lower troposphere but a much smaller increase in the low–middle troposphere (Fig. 11b and e).

Over the YRD, the enhanced vertical motions and increased precipitable water resulted in an increase in the rainfall at weaker intensity levels, although both the EASM-related moisture flux and local water vapour supply decreased. However, the development of deep convective activities was prohibited by a strong drying tendency in the lower troposphere. Consequently, significant changes were only detected for heavy storm rain, which resulted in the weakened DRAIN variability over urban areas of the YRD. However, changes in VRAIN for heavy storm rain were all significant over urban and nonurban areas and the entirety of YRD because of the corresponding changes in rainfall frequency and mean rain areas, showing the weakened VRAIN variability.

Over Shanghai, the increased moisture flux in the low–middle troposphere was similar to that over the YRD, whereas the decreased moisture flux in the lower troposphere was much stronger than the averaged values over the YRD. Therefore, the distributions for the changes in the moisture flux in the vertical direction accompanied by the decreased latent heat flux prohibited the development of deep convective systems, although the
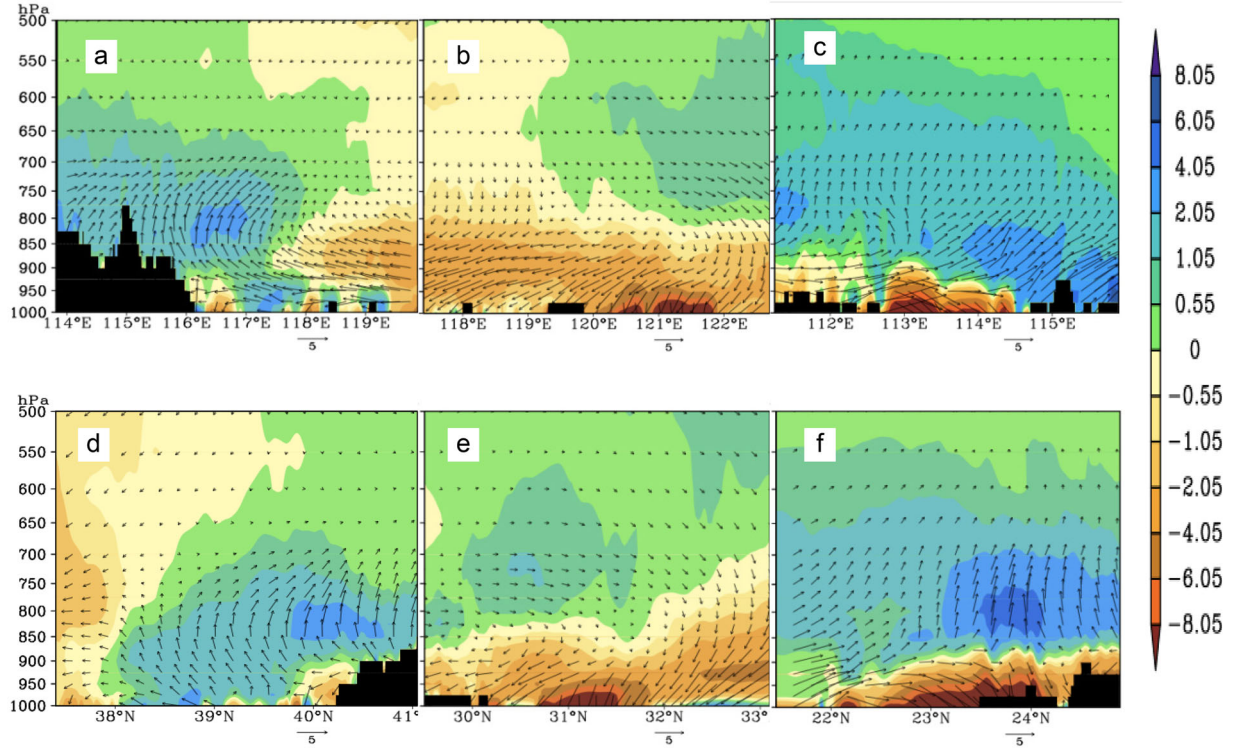
*Fig. 11.* Pressure (a–c) longitudinal and (d–f) latitudinal cross-sections along the (a) 39.9°N, (b) 31.14°N, (c) 23.08°N and (d) 116.3°E, (e) 121.29°E, (f) 113.14°E axes (black areas for topography) showing changes in the moisture flux (shaded) and vectors in the summer from U10 to U80 over the three city clusters of the (a, d) BTH, (b, e) YRD, and (c, f) PRD at 3.3-km resolution (units: $10^{-3}$ kg hPa$^{-1}$ m$^{-1}$ s$^{-1}$).

vertical motions were also enhanced. Consequently, the intensity of storm rain and heavy storm rain decreased, showing significant weakened DRAIN variability for storm rain and heavy storm rain over urban areas, and significant decreased DRAIN intensity for storm rain over urban and nonurban areas. The corresponding DRAIN for the weaker rainfall intensity levels generally increased but not significant. However, the corresponding changes in VRAIN were not significant.

*3.5.2.3. Over the PRD and Guangzhou.* Urban-induced changes in rainfall at various intensity levels in the summer displayed significant changes in DRAIN and VRAIN for the rainfall with both strong and weak intensities over the PRD and Guangzhou.

The EASM-related moisture flux expressed the southerly and southeasterly currents in the southern part but the southwesterly currents in the northern part, which was larger in the western but smaller in the eastern part (Fig. 9c). Urban-induced changes in moisture flux displayed the intensified currents across the entirety of PRD (Fig. 9f). The strengthened EASM-related moisture flux in the low–middle troposphere (Fig. 11c and f) could be interpreted by the increased wind speeds (Fig. 12c and f)

and water vapour mixing ratio (Fig. 13c and f). However, the weakened EASM-related moisture flux in the lower troposphere could be interpreted by the decreased wind speeds and water vapour mixing ratio. Overall, the precipitable water increased, especially over the northwestern part (Fig. 7f).

The enhanced vertical velocity, the decreased latent heat flux, and the generally increased moisture flux helped in the occurrences of the rainfall due to the abundant water vapour supply. However, the intense weakened moisture flux in the lower troposphere across both the PRD and Guangzhou prohibited the development of a deep convective system, hence the decreasing heavy storm rain. Consequently, significant changes in DRAIN over the PRD displayed the decreased DRAIN intensity for heavy storm rain but the increased DRAIN intensity for weaker rainfall. The corresponding changes in VRAIN were not significant. Meanwhile, significant changes in DRAIN over Guangzhou detected the weakened DRAIN variability for heavy storm rain and heavy rain but the increased DRAIN intensity for light rain. The corresponding significant changes in VRAIN showed the weakened VRAIN variability for heavy storm rain and increased VRAIN intensity for light rain.
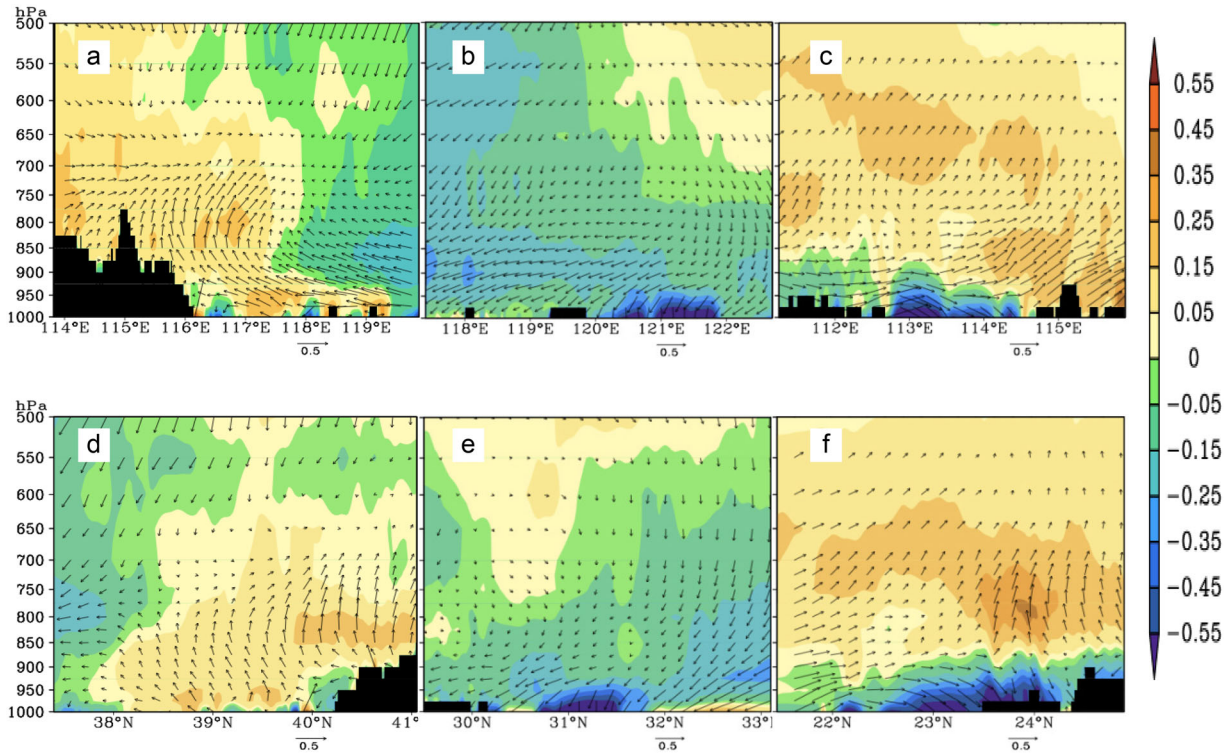
Fig. 12.    Pressure (a–c) longitudinal and (d–f) latitudinal cross-sections along the (a) 39.9°N, (b) 31.14°N, (c) 23.08°N and (d) 116.3°E, (e) 121.29°E, (f) 113.14°E axes (black areas for topography) showing changes in the wind speeds (shaded) and vectors in the summer from U10 to U80 over the three city clusters of the (a, d) BTH, (b, e) YRD, and (c, f) PRD at 3.3-km resolution (units: m s⁻¹).
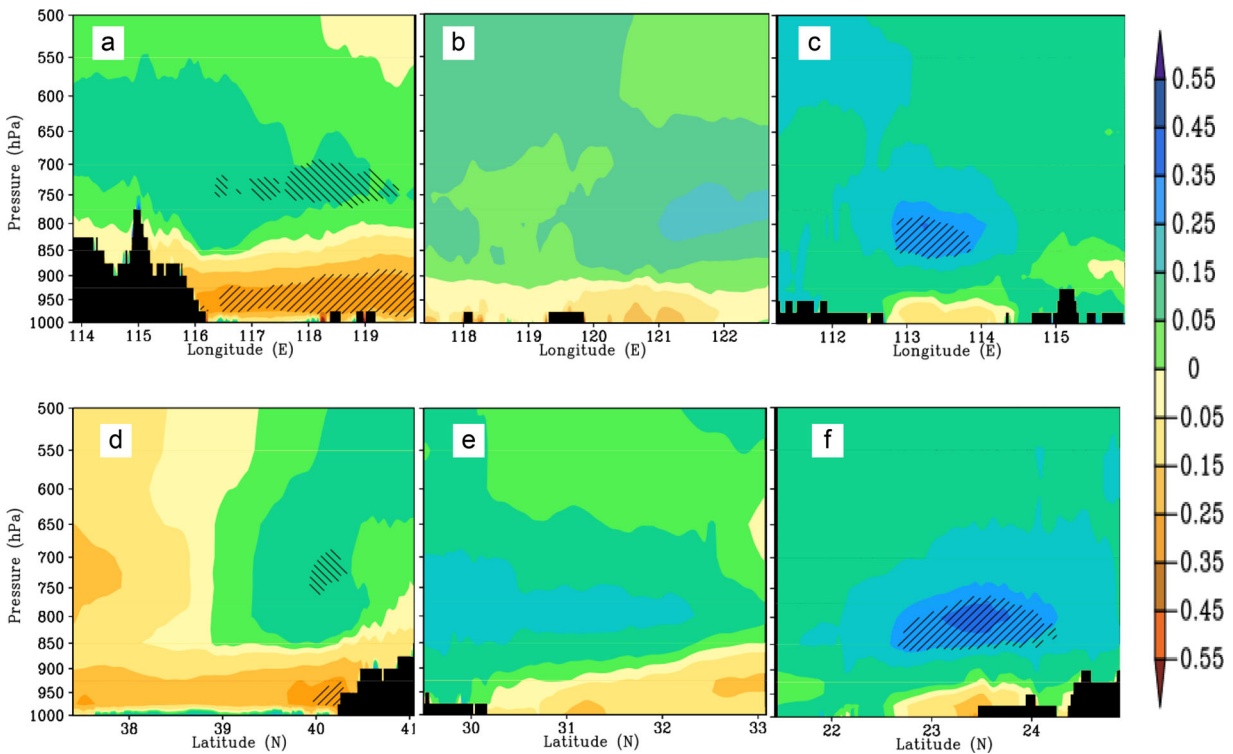
Fig. 13.    Same as Fig. 8, but for the results in the summer.

Overall, significant changes were observed in DRAIN and VRAIN for heavy storm rain, showing enhanced variability. Meanwhile, changes in DRAIN for light rain exhibited increased intensity.

## 4. Discussion

The present findings regarding urban-induced changes in rainfall are consistent with some previous conclusions based on both observed data and modelling result. With the data obtained from gauge stations or satellite observations, Zhang et al. (2014) found that the rainfall frequency decreased and the rainfall intensity increased over the urban areas of Beijing between 2000 and 2009, compared to its surrounding region. Contributions to total rainfall from strong rain increased after 2004 over Beijing (Yuan et al., 2017). The local rainfall increased because of the rapid development of urbanisation over the YRD between 1960 and 2005 (Lin and Sun, 2014) and Shanghai from 1979 and 2014 (Jin et al., 2017). Based on satellite data, Jiang and Tang (2011) found that rainfall increased over and downwind of the cities in the YRD from 2003 to 2009. Li et al. (2009) found that urban-induced changes in the rainfall were more likely to increase over urban areas of the PRD between 1998 and 2007. Urban-induced changes in total rainfall and the number of rain days for stronger rain have increased over Guangzhou since 1991 (Liao et al., 2011). Modelling results showed that the occurrences for the extreme precipitation increased in the urban area of Beijing during 2008 and 2012 (Yang et al., 2014). Urban-induced rainfall increased over the YRD from 2003 to 2007 (Zhang et al., 2010).

However, based on the observed data, Liang et al. (2011) found that both total rainfall and heavy storm rain increased over Shanghai between 1994 and 2007, while total rainfall decreased over the suburbs. Lin and Sun (2014) pointed out that the increase in total rainfall was due mainly to the increased strong rainfall over the YRD between 1960 and 2005. Simulations from Zhou et al. (2015) showed the decreasing tendency of the rainfall due to urbanisation over the BTH, YRD, and PRD between 1989 and 2009. Tan et al. (2018) showed that heavy storm rain and rain days decreased over the BTH but increased over the YRD and PRD between 1961 and 2014. Based on a case of storm rain, Wu and Tang (2011) found that the rainfall increased within and upwind of Shanghai while decreased over downwind areas.

Differences in changes in the daily and cumulative rainfalls at various levels of intensity between the observation and the simulation might have resulted from the sparse and short-period observations by station networks

(Jia et al., 2019). The spatial and temporal scales were key issues for both urban land–use changes as well as the climatic effects, which need to be considered when analysing the impacts of land–use changes on the climate.

At the spatial scale, studies on climatic effects at the city level revealed decreased albedo and increased surface roughness owing to urban surface expansion. Changes in the energy and water cycles at the local scale resulted in an increased average and strong rainfall over and downwind of the cities (Dou et al., 2014; McLeod et al., 2017; Liang and Ding, 2017). The risk of urban flooding was likely to increase (Shade and Kremer, 2019). Urban warming induced enriched water vapour in the atmosphere by influencing the hydrological cycle as well as strengthened or weakened dynamical characteristics. These induced further changes in the strong rainfall at the regional scales (Wu et al., 2013; Pfahl et al., 2017) through impacts on the energy and water cycles of the EAM climate system. The estimated contribution to centennial global warming due to urban land–use was less than 10%, whereas the impacts at the regional and local scales might have been much larger (IPCC, 2013), comparable to the impact of increasing greenhouse gases (Pitman et al., 2012). Therefore, urban studies should be performed not only at the individual city or city cluster level, but also over EAM regions, for which the impact on monsoon climate system is included.

At the temporal scale, urban changes in rainfall at various intensity levels depended on the periods of urban surface expansion (Jiang et al., 2011; Lin and Sun, 2014). Urban surface expansion in China mainly occurred from the 1980s, especially with the intense urbanisation after 2000s (Zhao and Wu, 2017). The calculated climatic effects from urban surface expansion might have varied with study period.

The calculated climatic effect could vary when the spatial and temporal scales of urban land–use differed. These scales for both urban land–use and the corresponding climatic effects should be addressed when exploring urban changes in rainfall at various intensity levels.

Changes in the daily and cumulative volumetric rainfalls at various levels of intensity due to urban surface expansion were explored using nested numerical experiments here. The second-nested domains covered the three city clusters (the BTH, YRD, and PRD), on which convection-permitting simulations were performed at the city scale. The coarse mesh covered the majority of East Asia, based on which the impacts on the energy and water cycles of the EAM climate systems were assesed at the regional scales. Therefore, urban changes in energy and water exchanges of the monsoon climate systems were detected at both the city and regional scales (including subgrid scales), in contrast to most previous studies

focusing on cities or city clusters (Changnon et al., 1991; Wu and Tang, 2015). Furthermore, convection-permitting simulations can help avoid uncertainties owing to different cumulus convective parameterisation schemes due to a coarse resolution. The modelled strong or extreme rainfall might be more reliable with convection-permitting simulations (Chawla et al., 2018).

Uncertainties still arose in several aspects of the numerical experiments. First, there were uncertainties in urban land–use and driving data, which varied significantly among different sources or methods. Second, uncertainties were present in certain regional climate models, such as descriptions of physical processes, physical parameters, and parameterisation schemes. Marked differences were observed in different RCMs. Third, characteristics of the subgrid scale on urban surface distributions and changes could not be captured by the second-nested domain grids (Li et al., 2013). The exchanges of energy and water between the land and atmosphere could not be adequately represented in the model grids, and have influenced the energy and water cycles of EAM climate systems. Finally, the simulation periods employed in the studies might also have resulted in uncertainties in changes in rainfall. Therefore, ensemble simulations with different urban land–use data, driving data, RCMs, parameterisation schemes, and with subgrid scale processes included might help reduce uncertainties in urban-induced changes in rainfall.

Marked differences were also detected among the numerical experiments, in which model resolution is an important issue when exploring the impacts of urban surface expansion. Although urbanisation in China has occurred rapidly in the past several decades, the urban areas accounted for only 2% of the total area of the country in 2017 (Gong et al., 2019). Therefore, the urban surface distribution and its expansion cannot be reproduced at a coarse resolution, such as 30 km (the urban area occupied by a city is usually less than $900\,km^2$). Fine-resolution simulations are necessary for studying the impacts of urbanisation. With the development of high-performance computing, model resolution has improved drastically, and can be used to perform studies at finer resolutions on the impacts of urbanisation, squall lines, and tornadoes, for instance. Consequently, using convection-permitting horizontal resolutions of less than 4 km is a good means of capturing DRAIN and VRAIN, which can reflect the urban surface expansion and avoid uncertainties due to cumulative convective parameterisation schemes. The horizontal resolution is adequately determined by the simulated domain, and studies at the city scale might be much finer, even at $10^1$–$10^2$ m, whereas those at country-wide scale might be coarser. Furthermore, with improvement in horizontal resolution

from reanalysis data or general circulation models, finer-resolution outputs can be made available for statistical downscaling, which is suitable for studying how urban surface expansion affects regional climate.

Studies on urban-induced changes in rainfall arrive at different conclusions when using different methods (observation data or simulation results), or spatial and temporal scales of interest. Considerable uncertainty persists about urban-induced changes in rainfall. More studies are needed, including ones to (i) obtain more gauge-based data with dense and long-term observation station networks or satellite-based data, (ii) describe the physical process of the numerical models more concisely, and (iii) use fine-resolution driving data and urban land–use data.

## 5. Conclusions

With the nested regional climate model and satellite-retrieved urban surface distributions between 1980s and 2010s, urban-induced changes in rainfall at various intensity levels were explored.

Significant urban-induced changes in variability in DRAIN/VRAIN and their intensities were detected over different spatial scales for various levels of intensity of rainfall, for which changes in rainfall variability were more distinct for stronger rainfall among rainfalls of various intensity levels whereas those in rainfall intensity were more pronounced for weaker rainfall. The changes in heavy storm rain were more distinct among rainfalls of various intensity levels, and the risk of the occurrence of heavy storm rain either increased or decreased with marked subregional dependence.

Urban-induced changes in DRAIN and VRAIN for total rainfall and rainfall at different intensity levels expressed marked subregional characteristics. Urban-induced changes in the rainfall could not be interpreted solely by enhanced vertical motions and decreased local water vapour supply. These changes in the EASM-related moisture flux in the vertical direction played an important role in determining subregional changes in the rainfall at various intensity levels, which were more pronounced for storm rain and heavy storm rain. The EASM-related moisture flux increased in the low–middle troposphere over the three city clusters, with high centres located over the three cities. However, the EASM-related moisture flux decreased in the lower troposphere over the three city clusters, especially over the three cities. Urban-induced drying tendency in the lower troposphere and the wetting tendency in the low–middle troposphere, and the enhanced vertical motions played an important role in determining changes in DRAIN and VRAIN for storm rain and heavy storm rain.

## Acknowledgement

## Disclosure statement

## Supplemental data

## References

Baik, J. J., Kim, Y. H., Kim, J. J. and Han, J. Y. 2007. Effects of boundary-layer stability on urban heat island-induced circulation. *Theor. Appl. Climatol.* **89**, 73–81. doi:10.1007/s00704-006-0254-4

Burian, S. J. and Shepherd, J. M. 2005. Effect of urbanization on the diurnal rainfall pattern in Houston. *Hydrol. Process.* **19**, 1089–1103. doi:10.1002/hyp.5647

Changnon, S. A., Semonin, R. G., Auer, A. H., Braham, R. R. and Hales, J. 1981. *METROMEX*: a review and summary. *Meteorol. Monogr.* **40**, 81.

Changnon, S. A., Shealy, R. T. and Scott, R. W. 1991. Precipitation changes in fall, winter, and spring caused by St. Louis. *J. Appl. Meteorol.* **30**, 126–134. doi:10.1175/1520-0450(1991)030<0126:PCIFWA>2.0.CO;2

Chawla, I., Osuri, K. K., Mujumdar, P. P. and Niyogi, D. 2018. Assessment of the Weather Research and Forecasting (WRF) model for simulation of extreme rainfall events in the upper Ganga Basin. *Hydrol. Earth Syst. Sci.* **22**, 1095–1117. doi:10.5194/hess-22-1095-2018

Chen, H., Zhang, Y., Yu, M., Hua, W., Sun, S. and co-authors. 2016. Large-scale urbanization effects on eastern Asian summer monsoon circulation and climate. *Clim. Dyn.* **47**, 117–136. doi:10.1007/s00382-015-2827-3

Chervin, R. M. and Schenider, S. H. 1976. On determining the statistical significance of climate experiments with general circulation models. *J. Atmos. Sci.* **33**, 405–322. doi:10.1175/1520-0469(1976)033<0405:ODTSSO>2.0.CO;2

Diem, J. E. 2008. Detecting summer rainfall enhancement within metropolitan Atlanta, Georgia USA. *Int. J. Climatol.* **28**, 129–133.

Dou, J., Wang, Y., Bornstein, R. and Miao, S. 2014. Observed spatial characteristics of Beijing urban climate impacts on summer thunderstorms. *J. Appl. Meteorol. Climatol.* **54**, 94–105.

Fu, C. B. 1997. Concept of "general monsoon system", an earth system science view on Asia monsoon. In: *Proceedings of the international workshop on regional climate modeling of the general monsoon system in Asia*, Beijing, China, pp. 1–6.

Gao, X. J., Xu, Y., Zhao, Z. C., Pal, J. S. and Giorgi, F. 2006. On the role of resolution and topography in the simulation of East Asia precipitation. *Theor. Appl. Climatol.* **86**, 173–185. doi:10.1007/s00704-005-0214-4

Gong, P., Li, X. C. and Zhang, W. 2019. 40-Year (1978–2017) human settlement changes in China reflected by impervious surfaces from satellite remote sensing. *Sci. Bull.* **64**, 756–763. doi:10.1016/j.scib.2019.04.024

Grell, G. A., Dudhia, J. and Stauffer, D. R. 1994. *A Description of the Fifth-Generation Penn State/NCAR Mesoscale Model (MM5)*. NCAR Technical Note NCAR/TN-398 + STR, NCAR, Boulder, CO, USA, 121 pp. doi:10.5065/D60Z716B.

Groisman, P. Y., Koknaeva, V. V., Belokrylova, T. A. and Karl, T. R. 1975. Overcoming biases of precipitation measurement: a history of the USSR experience. *Bull. Am. Meteorol. Soc.* **72**, 1725–1834.

Hayashi, Y. 1982. Confidence intervals of a climatic signal. *J. Atmos. Sci.* **39**, 1895–1905. doi:10.1175/1520-0469(1982)039<1895:CIOACS>2.0.CO;2

He, Y. T., Jia, G. S., Hu, Y. H. and Zhou, Z. J. 2013. Detecting urban warming signals in climate records. *Adv. Atmos. Sci.* **30**, 1143–1153. doi:10.1007/s00376-012-2135-3

Hu, Y. H., Jia, G. S., Pohl, C., Feng, Q., He, Y. T. and co-authors. 2015. Improved monitoring of urbanization processes in China for regional climate impact assessment. *Environ. Earth Sci.* **73**, 8387–8404. doi:10.1007/s12665-014-4000-4

Inoue, T. and Kimura, F. 2004. Urban effects on low-level clouds around the Tokyo metropolitan area on clear summer days. *Geophys. Res. Lett.* **31**, L05103.

IPCC. 2001. Climate change 2001: the scientific basis. In: *Contribution of Working Group I to the Third Assessment Report of the Intergovernmental Panel on Climate Change* (eds. J. T. Houghton, Y. Ding, D. J. Griggs, M. Noguer, P. J. van der Linden and co-editors). Cambridge University Press, Cambridge, United Kingdom and New York, NY, 881 pp.

IPCC. 2007. Climate change: the physical science basis. In: *Contribution of Working Group I to the Fourth Assessment Report of the Intergovernmental Panel on Climate Change* (eds. S. Solomon, D. Qin, M. Manning, Z. Chen, M., Margiquis

and co-editors). Cambridge University Press, Cambridge and New York, NY, 996 pp.

IPCC. 2013. Climate Change: the physical science basis. In: *Contribution of Working Group I to the Fifth Assessment Report of the Intergovernmental Panel on Climate Change* (eds. T. F. Stocker, D. Qin, G.-K. Plattner, M. Tignor, S. K. Allen and co-editors). Cambridge University Press, Cambridge, United Kingdom and New York, NY, 1535 pp.

Jia, G., Shevliakova, E., Artaxo, P., De Noblet-Ducoudré, N., Houghton, R. and co-authors. 2019. Land–climate interactions. In: *Climate Change and Land: An IPCC Special Report on Climate Change, Desertification, Land Degradation, Sustainable Land Management, Food Security, and Greenhouse Gas Fluxes in Terrestrial Ecosystems* (eds. P. R. Shukla, J. Skea, E. Calvo Buendia, V. Masson-Delmotte, H.-O. Pörtner and co-editors), 864 pp. In Press. Online at https://www.ipcc.ch/srccl/chapter/chapter-2/.

Jia, G. S., Xu, R. H., Hu, Y. H. and He, Y. T. 2014. Multi-scale remote sensing estimates of urban fractions and road widths for regional models. *Clim. Change* 129, 543–554.

Jiang, Z. H. and Tang, Z. F. 2011. Urbanization effects on precipitation over the Yangtze River Delta based on CMORPH data (in Chinese). *J. Meteorol. Sci.* 31, 355–364.

Jin, Y. R., Hu, Q. F., Wang, Y. T., Huang, Y., Yang, H. B. and co-authors. 2017. Impacts of rapid urbanization on precipitation at two representative rain gauges in Shanghai City (in Chinese). *J. Hohai Univ. (Nat. Sci.)* 45, 204–210.

Keuser, A. P. M. 2014. Precipitation patterns and trends in the metropolitan area of Milwaukee, Wisconsin. *Int. J. Geospatial Environ. Res.* 1, Article 6. Online at: https://dc.uwm.edu/ijger/vol1/iss1/6.

Kishtawal, C. M., Niyogi, D., Tewari, M., Pielke, R. A. and Shepherd, J. M. 2010. Urbanization signature in the observed heavy rainfall climatology over India. *Int. J. Climatol.* 30, 1980–1916.

Landsberg, H. E. 1956. The climate of towns. In: *Man's Role in Changing the Face of the Earth* (ed. W. L. Thomas), The University of Chicago Press, Chicago, IL, USA, pp. 584–606.

Landsberg, H. E. 1970. Man-made climatic changes: man's activities have altered the climate of urbanized areas and may affect global climate in the future. *Science* 170, 1265–1274. doi:10.1126/science.170.3964.1265

Li, D., Bou-Zeid, E., Barlage, M., Chen, F. and Smith, J. A. 2013. Development and evaluation of a mosaic approach in the WRF-Noah framework. *J. Geophy. Res.: Atmos.* 118, 11918–11935. doi:10.1002/2013JD020657

Li, W. B., Du, L. D. and Wang, G. D. 2009. Urbanization effects on precipitation over the Pearl River Delta based on satellite data (in Chinese). *Chin. J. Atmos. Sci.* 33, 1259–1266.

Liang, P. and Ding, Y. 2017. The long-term variation of extreme heavy precipitation and its link to urbanization effects in Shanghai during 1916–2014. *Adv. Atmos. Sci.* 34, 321–334. doi:10.1007/s00376-016-6120-0

Liang, P., Ding, Y. H., He, J. H. and Tang, X. 2011. Study of relationship between urbanization speed and change of spatial distribution of rainfall over Shanghai (in Chinese). *J. Trop. Meteorol.* 27, 475–483.

Liao, J. B., Wang, X. M., Li, Y. X. and Xia, B. C. 2011. An analysis study of the impacts of urbanization on precipitation in Guangzhou. *J. Meteorol. Sci.* 31, 384–390.

Lin, C.-Y., Chen, W.-C., Liu, S. C., Liou, Y. A., Liu, G. R. and co-authors. 2008. Numerical study of the impact of urbanization on the precipitation over Taiwan. *Atmos. Environ.* 42, 2934–2947. doi:10.1016/j.atmosenv.2007.12.054

Lin, H. and Sun, J. N. 2014. Possible effects of urbanization on regional precipitation over Yangtze River Delta area (in Chinese). *J. Nanjing Univ. (Nat. Sci.)* 50, 792–799.

Ma, H., Jiang, Z., Song, J., Dai, A., Yang, X. and co-authors. 2016. Effects of urban land-use change in East China on the East Asian summer monsoon based on the CAM5.1 model. *Clim. Dyn.* 46, 2977–2989. doi:10.1007/s00382-015-2745-4

Ma, X. and Zhang, Y. 2015. Numerical study of the impacts of urban expansion on Meiyu precipitation over Eastern China. *J. Meteorol. Res.* 29, 237–256. doi:10.1007/s13351-015-4063-5

McAnelly, R. L., Nachamkin, J. E., Cotton, W. R. and Nicholls, M. E. 1997. Upscale evolution of MCSs: Doppler radar analysis and analytical investigation. *Monthly Weather Rev.* 125, 1083–1110. doi:10.1175/1520-0493(1997)125<1083:UEOMDR>2.0.CO;2

McLeod, J., Shepherd, M. and Konrad, C. E. 2017. Spatio-temporal rainfall patterns around Atlanta, Georgia and possible relationships to urban land cover. *Urban Clim.* 21, 27–42. doi:10.1016/j.uclim.2017.03.004

Meng, Y. F., Sun, Y. G., Sarina, Yuan and Hasi. 2013. Correlation between eastward developing of hetao cyclone and the severe rainstorm in Beijing on 21 July 2012 (in Chinese). *Meteorol. Monthly* 39, 1542–1549.

Mote, T. L., Lacke, M. C. and Shepherd, J. M. 2007. Radar signatures of the urban effect on precipitation distribution: a case study for Atlanta, Georgia. *Geophys. Res. Lett.* 34, 1–4.

Niyogi, D., Pyle, P., Lei, M., Arya, S. P., Kishtawal, C. M. and co-authors. 2011. Urban modification of thunderstorms: an observational storm climatology and model case study for the Indianapolis urban region. *J. Appl. Meteorol. Climatol.* 50, 1129–1144. doi:10.1175/2010JAMC1836.1

Niyogi, D., Lei, M., Kishtawal, C., Schmid, P. and Shepherd, M. 2017. Urbanization impacts on the summer heavy rainfall climatology over the eastern United States. *Earth Interact.* 21, 1–17. EI-D-15-0045.1.

Pfahl, S., O'Gorman, P. A. and Fischer, E. M. 2017. Understanding the regional pattern of projected future changes in extreme precipitation. *Nat. Clim. Change* 7, 423–427. doi:10.1038/nclimate3287

Pitman, A. J., de Noblet-Ducoudre, N., Avila, F. B., Alexander1, L. V., Boisier, J.-P. and co-authors. 2012. Effects of land cover change on temperature and rainfall extremes in multi-model ensemble simulations. *Earth Syst. Dyn.* 3, 231–231.

Shade, C. and Kremer, P. 2019. Predicting land use changes in Philadelphia following green infrastructure policies. *Land* 8, 28. doi:10.3390/land8020028

Shepherd, J. M., Pierce, H. and Negri, A. J. 2002. Rainfall modification by major urban areas: observations from spaceborne rain radar on the TRMM satellite. *J. Appl.*

*Meteorol.* **41**, 689–701. doi:10.1175/1520-0450(2002)041<0689:RMBMUA>2.0.CO;2

Tan, C., Kong, F., Guo, J., Lu, L. and Sun, S. 2018. Spatial and Temporal patterns of heavy rainfall in different urbanized areas of China from 1961-2014: taking Beijing-Tianjin-Hebei, Yangtze River Delta and Pearl River Delta as an Example (in Chinese). *J. Gatastrophol.* **33**, 132–139.

Tayanc, M., Karaca, M. and Yenigün, O. 1997. Annual and seasonal air temperature trend patterns of climate change and urbanization effects in relation to air pollutants in Turkey. *J. Geophys. Res.* **102**, 1909–1920. doi:10.1029/96JD02108

Weaver, C. P. and Avissar, R. 2001. Atmospheric disturbances caused by human modification of the landscape. *Bull. Am. Meteorol. Soc.* **82**, 269–228. doi:10.1175/1520-0477(2001)082<0269:ADCBHM>2.3.CO;2

Wu, F. B. and Tang, J. P. 2011. The impact of urbanization on a heavy rainfall case in Shanghai on 25 August 2008. *J. Nanjing Univ. (Nat. Sci.)* **47**, 71–81.

Wu, F. B. and Tang, J. P. 2015. The impact of urbanization on summer precipitation and themperature in the Yangtze River Delta. *J. Trop. Meteorol.* **31**, 255–263.

Wu, P., Christidis, N. and Stott, P. 2013. Anthropogenic impact on Earth's hydrological cycle. *Nat. Clim. Change* **3**, 807–810. doi:10.1038/nclimate1932

Yan, Z. W., Li, Z., Li, Q. X. and Jones, P. 2010. Effects of site change and urbanisation in the Beijing temperature series 1977-2006. *Int. J. Climatol.* **30**, 1226–1234.

Yang, L., Tian, F. Q., Smith, J. A. and Hu, H. 2014. Urban signatures in the spatial clustering of summer heavy rainfall events over the Beijing metropolitan region. *J. Geophys. Res. Atmos.* **119**, 1203–1217. doi:10.1002/2013JD020762

Yao, X. X. and Xu, J. 2004. A study of volumetric precipitation during the Huaihe river basin floods in 2003 (in Chinese). *Acta Meteorol. Sin.* **62**, 803–813.

Yuan, Y. F., Zhai, P. M., Li, Y. and Chen, Y. 2017. Changes in classified precipitation in the urban, suburban and mountain areas of Beijing. *Clim. Change Res.* **13**, 589–598.

Zhang, N., Gao, Z. Q., Wang, X. M. and Chen, Y. 2010. Modeling the impact of urbanization on the local and regional climate in Yangtze River Delta, China. *Theor. Appl. Climatol.* **102**, 331–342. doi:10.1007/s00704-010-0263-1

Zhang, Y., Smith, J. A., Luo, L., Wang, Z. and Baeck, M. L. 2014. Urbanization and rainfall variability in the Beijing metropolitan region. *J. Hydrometeorol.* **15**, 2219–2235. doi:10.1175/JHM-D-13-0180.1

Zhao, D. M. and Wu, J. 2017. The influence of urban surface expansion in China on regional climate. *J. Clim.* **30**, 1061–1080. doi:10.1175/JCLI-D-15-0604.1

Zhao, D. M. and Wu, J. 2018. Changes in urban-related precipitation in the summer over three city clusters in China. *Theor. Appl. Climatol.* **134**, 83–93. doi:10.1007/s00704-017-2256-9

Zhong, S., Qian, Y., Zhao, C., Leung, R., Wang, H. and co-authors. 2017. Urbanization-induced urban heat island and aerosol effects on climate extremes in the Yangtze River Delta region of China. *Atmos. Chem. Phys.* **17**, 5439–5457. doi:10.5194/acp-17-5439-2017

Zhou, L., Dickinson, R. E., Tian, Y., Fang, J., Li, Q. and co-authors. 2004. Evidence for a significant urbanization effect on climate in China. *Proc. Natl. Acad. Sci. USA* **101**, 9540–9544. doi:10.1073/pnas.0400357101

Zhou, L., Jiang, Z. H., Lim, Z. X. and Yang, X. Q. 2015. Numerical simulation of urbanization climate effects in regions of East China (in Chinese). *Chin. J. Atmos. Sci* **39**, 596–610.